The University of Alberta
Printing Department
Edmonton, Alberta

THE UNIVERSITY OF ALBERTA

NMR STUDY OF THE RUDERMAN-KITTEL INTERACTION IN WHITE TIN USING MACROSCOPIC ROTATION

BY

© DAVID A. M. SWITZER

A THESIS

SUBMITTED TO THE FACULTY OF GRADUATE STUDIES AND RESEARCH

IN PARTIAL FULFILMENT OF THE REQUIREMENTS FOR THE DEGREE

OF MASTER OF SCIENCE

DEPARTMENT OF PHYSICS

EDMONTON, ALBERTA

FALL, 1973

ABSTRACT

This thesis describes a study of the rotationally invariant part of the electron-coupled nuclear spin-spin interaction, otherwise known as the Ruderman-Kittel interaction, in β (or white) tin. It is a continuation of the NMR study initiated in our laboratory by Smith (1972), in which the anisotropic nuclear spin interactions in β-tin are averaged by rotating a sample of tin powder at high speed using an air turbine. Provided the axis of rotation makes the so-called magic angle ($\cos^{-1} 1/\sqrt{3}$) with the external magnetic field, the broadening associated with the anisotropic interactions is completely removed and the NMR lineshape is governed by the Ruderman-Kittel interaction together with spin-lattice relaxation. The theoretical lineshape is synthesized and the strength of the Ruderman-Kittel interaction is obtained by fitting the theoretical lineshape to the experimental resonance.

Improvements made to the air turbine designed by Smith enabled us to record the Sn^{117} NMR signal with a greatly improved signal-to-noise ratio. The theoretical lineshape calculations made by Smith have been extensively revised and fewer approximations have been made. Also, a new fitting procedure has been developed which enables a theoretical lineshape which is computed numerically to be fitted to an experimental lineshape.

Agreement between experiment and a theoretical model, which assumes that only nearest neighbour spin-spin interactions are signi-

ficant, is very poor. Similarly, a model in which only second nearest neighbour interactions are non-zero, has been shown to be untenable. However, very good agreement has been obtained with the so-called Ruderman-Kittel model and we find that the strength of the interaction between nearest neighbour Sn^{117} and Sn^{119} nuclei is 3.04 ± 0.3 kHz. A comparison is made with other published values of this quantity.

Acknowledgements

I would like to express my sincere thanks to Dr. D. G. Hughes for suggesting this work. His interest and guidance during this project were much appreciated.

I would like to thank Dr. M. R. Smith, who did the original work on this subject, for his valuable discussions. Also I would like to thank Mr. P. Spencer for many helpful discussions and assistance.

I wish to acknowledge the assistance of members of the technical staff during this project.

I would like to thank the Unviersity of Alberta for the award of a GTA Scholarship and the National Research Council for the award of a Graduate Scholarship.

TABLE OF CONTENTS

LIST OF TABLES

LIST OF FIGURES

I INTRODUCTION

I(i) General

It has been known since the early work of Bloembergen and Rowland (1953) that the NMR linewidth of nuclei with I=1/2 cannot be wholly accounted for by direct nuclear magnetic dipole-dipole interactions and by a lifetime-limiting effect associated with spin-lattice relaxation. By measuring the Tl^{203} and Tl^{205} linewidths in various samples of thallium metal with different isotopic composition, Bloembergen and Rowland (1955) showed that an indirect interaction occurs between nuclear spins via the intermediary of the conduction electrons. In particular, they showed that the indirect interaction between two spins $\underline{I}_1$ and $\underline{I}_2$ consists of a scalar or rotationally invariant part of the form $J\underline{I}_1 \cdot \underline{I}_2$, sometimes given the name of pseudo-exchange interaction, together with a smaller anisotropic part, sometimes called the pseudo-dipolar interaction. A theory of the rotationally invariant part has been given by Ruderman and Kittel (1954), and indeed this interaction is also often called the Ruderman-Kittel interaction, a name which we shall adopt in this thesis.

The Ruderman-Kittel interaction between unlike neighbours contributes to the second moment of the NMR line (Ruderman and Kittel, 1954) and hence broadens it. On the other hand, the Ruderman-Kittel interaction between like neighbours leaves the second moment unaffected but increases the fourth and higher (even) moments. This implies a sharpening of the central part of the

resonance, a phenomenon called exchange narrowing.

The study of the indirect nuclear spin-spin interaction is important on two counts:

1) It provides an understanding of the factors which contribute to the width and shape of NMR lines in general.

2) It provides information regarding the hyperfine interaction between the nuclear spins and conduction electrons in metals.

There is some uncertainty in the magnitude of the Ruderman-Kittel interaction in the case of white or β-tin, since all the methods used so far have required a knowledge of the second moment of the tin resonance. Values for the magnitude of the Ruderman-Kittel interaction between Sn^{117} and Sn^{119} nuclei which occupy nearest neighbour sites in β-tin range from 2.0 ± 0.5 kHz obtained by McLachlan (1968) to 4.1 ± .3 kHz obtained by Alloul and Deltour (1969). A method has recently been described by Smith (1972) and uses the so-called magic angle, high-speed rotation technique. This involves rotating the sample at high speed (in practice at several kHz) about an axis making an angle $\cos^{-1}(1/\sqrt{3})$ with the external magnetic field.

In this thesis we describe some additional work done on this problem. In particular, substantial refinements to the theory given by Smith (1972) are presented together with a description of improved rotors which enable a much better signal-to-noise ratio to be achieved. Also, a better procedure for fitting theoretical lineshapes to experimental resonances is described.

In sections I(ii) and I(iii) of this thesis, a simple pic-

ture of NMR and a discussion of the magic angle, high-speed rotation technique are given. Section II contains the theoretical background for this thesis. In section III a discussion of the equipment and experimental method are given. In section IV the fitting procedure is described and the results are presented and discussed.

I(ii) A Simple Picture of NMR

Purcell, Torrey and Pound, (1946) and Bloch, Hansen and Packard (1946) carried out the first spin resonance experiments on nuclei in liquids and solids. When a nucleus with spin quantum number I is subjected to a steady magnetic field $\underline{H}_o$, there are 2I+1 equally spaced magnetic energy levels, with a separation

$$\Delta E = \mu H_o/I = \gamma\hbar H_o \qquad (1)$$

between adjacent energy levels. Here $\mu = \gamma\hbar I$ is the maximum z component of the nuclear magnetic moment ($\hat{z}$ is taken to be in the same direction as $\underline{H}_o$) and γ is the gyromagnetic ratio of the nucleus. If a group of nuclei which interact negligibly with each other are allowed to come to equilibrium with a heat reservoir at temperature T, a net magnetization, M_z, in the z direction is established which obeys the well known Curie law $M_z \propto 1/T$. When an rf magnetic field of frequency

$$\omega_o = \gamma H_o \qquad (2)$$

is applied perpendicular to $\underline{H}_o$, there is a net absorption of energy from the rf field with a new equilibrium value of M_z. Because

of the finite lifetime of the magnetic energy levels due to the interaction with the heat reservoir, there is also absorption of energy from the rf field for frequencies close to ω_o. For a group of spin 1/2 nuclei which interact only with a heat reservoir, the shape of the absorption spectrum is Lorentzian, the half-width of the spectrum being equal to $2W/\pi$, where $W = 1/2T_1$ is the transition rate and T_1 is the spin-lattice relaxation time.

For solids, the direct magnetic dipole-dipole interaction between nuclei is important (Van Vleck, 1948). Classically, the dipole-dipole interaction can be considered in the following way. Each nuclear magnet finds itself not only in the applied steady magnetic field $\underline{H}_o$, but also in a small local field $\underline{H}_{loc}$ produced by neighbouring nuclear moments. The magnitude and direction of $\underline{H}_{loc}$ differs from nuclear site to nuclear site, depending on the relative disposition of their magnetic quantum number m (where m can take on values -I, -I+1,...,I). The distribution of H_{loc} has a mean value of zero and a width of the order μ/r^3 where r is the nearest neighbour distance. As the resonance frequency of each nucleus takes on different values due to the variation in $\underline{H}_{loc}$, the resonance will be further broadened (in addition to lifetime broadening).

In a metal, another important interaction is that between nuclear spins and the electronic spins. A simple way to examine this is to consider the magnetic field produced by electronic spins. This rapidly fluctuating field can be divided into its time-average and the difference between the time-average and the value of the

field at a given time. The time-averaged field, which to a good approximation is parallel to $\underline{H}_o$, causes a shift ΔH of the resonance which is proportional to H_o (and usually down field). This shift was first observed by Knight (1949) and the so-called Knight Shift K is defined as $\Delta H/H_o$. When the time-averaged distribution of the electrons about a nuclear site has lower than cubic (or tetrahedral) symmetry, the Knight Shift is anisotropic, that is it depends on the orientation of the metal with respect to $\underline{H}_o$. It can be shown that the Knight Shift is a second rank tensor. This is a further source of broadening when the sample is in the form of a powder since the various grains of the powder will have different orientations with respect to $\underline{H}_o$. The time-dependent magnetic field caused by the electronic spins gives rise to a spin-lattice relaxation.

A second effect of the time-averaged magnetic field is the indirect interaction which was previously mentioned in section I(i). The existence of such an interaction can be visualized by the following picture (Slichter, 1963). Consider two magnetic nuclei amongst non-magnetic nuclei. The effect of the spin of one of the nuclei is, in general, to make the nuclear site more favourable for an electron with a spin parallel to the magnetic moment of the nucleus. The zero states of the electrons are Bloch states and in order to increase the probability of an electron with a negative spin orientation being in the vicinity of a nuclear site of negative magnetic moment, it is necessary to mix Bloch states of negative spin orientation and with wavevector k greater than the Fermi wavevector k_f (because of the exclusion principle). These Bloch states are in

phase at the nuclear site but become progressively more out of phase with increasing distance from the magnetic nucleus. This implies that the conduction electron density oscillates about the average value. The magnitude of the oscillations decreases with increasing distance. Consequently, the second magnetic nucleus experiences a different time-averaged magnetic field, thereby giving rise to an interaction.

There is also a nuclear quadrupole interaction but this interaction does not occur in tin as the magnetic isotopes of tin have a spin of 1/2. As a result we will not describe this interaction.

I(iii) Macroscopic Rotation

The first studies using the sample rotation technique were made by Andrew et al (1958) to confirm the theoretical predictions of Anderson (1954) and Pake (1956) that hindered rotation in a solid should not cause a reduction in the second moment of the NMR spectrum. When they rotated the sample as a whole, Andrew et al found that the central part of the spectrum was narrowed but sidebands appeared in such a way that the second moment remained invariant. Narrowing by macroscopic rotation at the magic angle has been studied in more detail by Andrew and Newing (1958), Andrew and Jenks (1962) and Schwind (1967). It has been shown by Kessemeier (1967) that if the rate of rotation is much greater than the NMR linewidth of the stationary sample, the central part of the resonance is resolved from the sidebands, and only the time-averaged interactions need be

included in the Hamiltonian to study the central part. A comprehensive study has been undertaken by Andrew and Farnell (1968) in connection with the averaging of anisotropic interactions by rotation.

II THEORY

II(i) General

The Hamiltonian of a group of nuclear spins interacting with a 'thermal bath' of conduction electrons in a metal can be written as

$$\mathcal{H} = \hbar E + \hbar F + \hbar Q \qquad (1)$$

where $\hbar E$ involves only the nuclei, $\hbar F$ involves only the thermal bath and $\hbar Q$ is the interaction between the nuclei and thermal bath. Q can be written as

$$Q_{\alpha f u \alpha' f' u'} = \sum_q K^q_{\alpha\alpha'} H^q_{fuf'u'} \qquad (2)$$

where α,α' are eigenvalues of E, and f,f' are eigenvalues of F of degeneracy u and u' respectively; K^q is an observable of the nuclei and H^q is an observable of the thermal bath. For a metal we have

$$\hbar Q = \sum_i a_i \underline{I}_i \cdot \sum_\ell \underline{S}_\ell \delta(\underline{r}_{i\ell} - \underline{R}_i) + \sum_i b_i \underline{I}_i \cdot \sum_\ell \underline{\underline{D}}_{\ell i} \cdot \underline{S}_\ell + \sum_i c_i \underline{I}_i \cdot \sum_\ell \underline{L}(\underline{r}_{i\ell}) / r_{i\ell}^3 \qquad (3)$$

where $a_i = 8\pi\gamma_e\gamma_i\hbar^2/3$, $b_i = \gamma_e\gamma_i\hbar^2$, $c_i = 2\gamma_e\gamma_i$, $\underline{\underline{D}}_{\ell i} = \sum_\ell 1/\{|\underline{r}_{i\ell} - \underline{R}_i|^3 - (\underline{r}_{i\ell} - \underline{R}_i)\cdot(\underline{r}_{i\ell} - \underline{R}_i)/|\underline{r}_{i\ell} - \underline{R}_i|^5\}$ and γ_i and γ_e are the gyromagnetic ratios of the ith nucleus and an electron respectively. $\underline{L}(\underline{r}_{i\ell})$ is the angular momentum operator for the ℓth electron with respect to the ith nucleus as center and $\underline{r}_{i\ell}$ is the position vector for the ℓth electron with respect to the ith nucleus (Das and Mahanti, 1968). The first term in (3) is the so-called Fermi contact interaction and the second term describes the dipolar interaction between the nuclear spins and the electron spins.

The density matrix operator (Davydov, 1966 p. 42) for the

nuclei and the bath is ρ and is assumed to be of the form (Redfield, 1957)

$$\rho_{\alpha fu\alpha' fu'}(t) = \sigma_{\alpha\alpha'}(t)P(f)\delta_{ff'}\delta_{uu'} \tag{4}$$

with

$$P(f) = \exp(-\hbar f/kT)/\Sigma'_{fu}\exp(-\hbar f'/kt). \tag{5}$$

Redfield found that

$$d\sigma/dt \equiv (\sigma(t+\Delta t)-\sigma(t))/\Delta t = i[\sigma,E+M+N] + R \tag{6}$$

if $\Delta t >> \tau_c$, and $M,N,R << 1/\tau_c < kT/\hbar$, where τ_c can be thought of as the classical correlation time for the random magnetic fields produced at the nuclear sites by the electrons. Redfield showed that the matrix elements of the operators M and N are

$$M_{\alpha\alpha'} = \Sigma_q K^q_{\alpha\alpha'} \Sigma_{fu} H^q_{fufu} P(f) \tag{7}$$

$$N_{\alpha\alpha'} = \Sigma_\gamma \Sigma_{qq'} K^{q'}_{\gamma\alpha'} K^q_{\alpha\gamma} \pi \int_{-\infty}^{\infty} d\omega \; j_{qq'}(-\omega)/(\tfrac{1}{2}\alpha+\tfrac{1}{2}\alpha'-\gamma-\omega) \quad . \tag{8}$$

Also he found that

$$(R'\sigma)_{\alpha\alpha'} = \Sigma_{\beta\beta'} R'_{\alpha\alpha'\beta\beta'}\sigma_{\beta\beta'} \tag{9}$$

and

$$R'_{\alpha\alpha'\beta\beta'} = \Sigma_{qq'}\{K^q_{\alpha\beta}K^{q'}_{\beta\alpha'}(j_{qq'}(\alpha-\beta)+j_{qq'}(\alpha'-\beta')) - \tag{10}$$

$$\delta_{\alpha\beta}\Sigma_\gamma K^q_{\beta\gamma}K^{q'}_{\gamma\alpha'} j_{qq'}(\beta'-\gamma)e^{\hbar(\beta'-\gamma)/kT} - \delta_{\alpha'\beta'}\Sigma_\gamma K^q_{\alpha\gamma}K^{q'}_{\gamma\beta} j_{qq'}(\beta-\gamma)e^{\hbar(\beta-\gamma)/kT}$$

where

$$j_{qq'}(\omega) = \pi \int_{-\infty}^{\infty} df \; \{\Sigma'_{uu'} P(f)H^q_{(f-\omega)ufu'}H^{q'}_{fu'(f-\omega)u}\eta_u(f-\omega)\eta_{u'}(f)\}$$

and $\eta_u(f)$ is the density of states for eigenvalue f and degeneracy u. In writing (10), Redfield assumed that only secular terms con-

tributed to $R'_{\alpha\alpha'\beta\beta'}$, that is only terms where $\alpha-\alpha'-\beta+\beta' = 0$. However, for non-secular terms, Redfield showed that one must multiply the right hand side of (10) by a term of the form

$$A_{\alpha\alpha'\beta\beta'} = \{e^{i(\alpha-\alpha'-\beta+\beta')\Delta t}-1\}/(\alpha-\alpha'-\beta+\beta')\Delta t . \qquad (11)$$

M can be identified with the Knight Shift operator (K^q in (2) is taken to be one of the components of the spin operator for one of the nuclei because of (3)) and N is the indirect spin-spin interaction operator (ignoring terms in (8) where q and q′ refer to the same nuclear spin). The R' operator is the relaxation operator.

The operator $\hbar(E+M+N)$ can therefore be expressed as

$$-\hbar\Sigma_i \gamma_i \underline{I}_i \cdot (\underline{\underline{1}}+\underline{\underline{K}})\cdot \underline{H}_o + h \sum_{i<j} \underline{I}_i \cdot (\underline{\underline{J}}_{ij} + \underline{\underline{D}}_{ij}) \cdot \underline{I}_j \qquad (12)$$

where $\underline{\underline{K}}$ is the Knight Shift tensor, and $\underline{\underline{J}}_{ij}$ and $\underline{\underline{D}}_{ij}$ are respectively the indirect tensor and the dipolar interaction tensor between nuclei i and j. It follows that (6) can be written in the form

$$d\sigma/dt = i\left[\sigma, (-\Sigma_i \gamma_i \underline{I}_i \cdot (\underline{\underline{1}}+\underline{\underline{K}})\cdot \underline{H}_o + 2\pi \sum_{i<j} \underline{I}_i \cdot (\underline{\underline{J}}_{ij}+\underline{\underline{D}}_{ij})\cdot \underline{I}_j)\right] + R'\sigma , \qquad (13)$$

II(ii) Effect of Macroscopic Rotation on $\underline{\underline{K}}$, $\underline{\underline{J}}$, and $\underline{\underline{D}}$

Because of the short correlation time of the conduction electrons ($\tau_c \simeq 10^{-11}$ seconds) and the fact that the period of the macroscopic rotation is typically 10^{-4} seconds, we can allow $\underline{\underline{K}}$, $\underline{\underline{J}}$ and $\underline{\underline{D}}$ in (13) to be time dependent. However, as pointed out in I(iii), the shape of the central part of the resonance is governed by the time-average of $\underline{\underline{K}}$, $\underline{\underline{D}}$ and $\underline{\underline{J}}$. The R operator in (13) is assumed to be unaffected by macroscopic rotation, since McLachlan (1968) found that the T_1 of Sn^{119} in β-tin was essentially independent of crystal orientation (the connection between T_1 and R is established in section II(iv)).

To find the time-averaged operators, it is noted that the interactions involving $\underline{\underline{K}}$, $\underline{\underline{J}}$ and $\underline{\underline{D}}$ are of the form $\underline{A}\cdot\underline{\underline{T}}\cdot\underline{B}$ where $\underline{A}$ and $\underline{B}$ are time independent vectors. Because of the symmetry of the crystal structure of β-tin, $\underline{\underline{T}}$ must be symmetric matrix (Smith, 1972, p. 94). Following Andrew and Farnell (1968), we can decompose the tensor into two parts, $\underline{\underline{T}}'$ and $\underline{\underline{T}}^*$, where $\underline{\underline{T}}'$ is equal to $(1/3)\mathrm{Tr}(\underline{\underline{T}})\underline{\underline{1}}$ and $\underline{\underline{T}}^*$ is a traceless tensor equal to $\underline{\underline{T}} - \underline{\underline{T}}'$. Because $\underline{\underline{T}}^*$ is symmetric

$$\underline{A}\cdot\underline{\underline{T}}^*\cdot\underline{B} = \sum_{\alpha\beta} T^*_{\alpha\beta} A_\alpha B_\beta = \sum_{\alpha\beta n} C_{\alpha n} C_{\beta n} T^*_n A_\alpha B_\beta \qquad (14)$$

where $C_{\alpha n}$ and $C_{\beta n}$ are the direction cosines between the axes x, y and z fixed with respect to the laboratory (represented in (14) by the indices α and β) and the principal axes of the tensor. The T_n's are the principal values of the tensor $\underline{\underline{T}}^*$. Using the relations $A_+ = A_x + iA_y$ and $A_- = A_x - iA_y$ plus similar relations for B_+ and B_-, we obtain

$$\underline{A}\cdot\underline{\underline{T}}^{*}\cdot\underline{B} = \Sigma T_n (D_n+E_n+F_n+H_n+I_n) \tag{15}$$

where

$$D_n = C_{3n}^2 A_z B_z$$

$$E_n = (1/4)(A_+B_- + A_-B_+)(C_{1n}^2 + C_{2n}^2)$$

$$F_n = (1/2)(C_{1n}C_{3n} - iC_{2n}C_{3n})(A_+B_z + A_zB_+)$$

$$G_n = (1/2)(C_{1n}C_{3n} + iC_{2n}C_{3n})(A_-B_z + A_zB_-)$$

$$H_n = (1/4)(C_{1n}^2 - 2iC_{1n}C_{2n} - C_{2n}^2)A_+B_+$$

$$I_n = (1/4)(C_{1n}^2 + 2iC_{1n}C_{2n} - C_{2n}^2)A_-B_- .$$

We now consider the truncated part of (15), that is, we consider the terms D_n and E_n. We can ignore the remaining terms when $\underline{A}$ and $\underline{B}$ represent spin vectors since these terms give rise to weak resonances at frequencies 0, $2\omega_o$, and $3\omega_o$, resonances which we are not interested in. We have

$$\begin{aligned}\Big(\sum_{\alpha\beta} T_n C_{\alpha n} C_{\beta n} A_\alpha B_\beta\Big)^{\text{trunc}} &= \Sigma T_n\{C_{3n}^2 A_z B_z + (1/4)(A_+B_- + A_-B_+)(C_{1n}^2+C_{2n}^2)\}\\ &= \Sigma T_n\{C_{3n}^2 A_z B_z + (1/2)(A_xB_x + A_yB_y)(1-C_{3n}^2)\}\\ &= \Sigma T_n(-1/2)C_{3n}^2(A_xB_x + A_yB_y - 2A_zB_z), \end{aligned}\tag{16}$$

In appendix I we show that the time-averaged value of C_{3n}^2 is 1/3 if the magic angle condition is satisfied. Since $\underline{\underline{T}}^{*}$ is traceless and $\overline{C_{3n}^2}$ is 1/3, the right hand side of (16) reduces to zero. Thus we have

$$\overline{(\underline{A}\cdot\underline{\underline{T}}^{*}\cdot\underline{B})^{\text{trunc}}} = 0. \tag{17}$$

If truncation is justified, then the time-averaged interaction (when the magic angle condition is satisfied) reduces to

$$\overline{\underline{A}\cdot\underline{\underline{T}}'\cdot\underline{B}} = (\underline{A}\cdot\underline{B})(1/3)\mathrm{Tr}(\underline{\underline{T}}). \tag{18}$$

For the dipolar interaction, $\underline{A}$ and $\underline{B}$ are spin vectors, and truncation is justified. Moreover, the dipolar interaction tensor is traceless. As a result, the time-averaged interaction is equal to zero.

The indirect interaction between nuclei can also be written in the form $\underline{A}\cdot\underline{\underline{T}}\cdot\underline{B}$, where $\underline{A}$ and $\underline{B}$ are spin operators. As a result the time-averaged indirect interaction becomes

$$\overline{\sum_{i<j} \underline{I}_i \cdot \underline{\underline{J}}_{ij} \cdot \underline{I}_j} = \sum_{i<j} J_{ij} \underline{I}_i \cdot \underline{I}_j \tag{19}$$

where $J_{ij} = (1/3)\mathrm{Tr}(\underline{\underline{J}}_{ij})$.

Finally, the Zeeman interaction can be written in the form $\underline{A}\cdot\underline{\underline{T}}\cdot\underline{B}$. However $\underline{A}$ is a nuclear spin vector and $\underline{B}$ is the steady magnetic field $\underline{H}_o$ in this case. The sum of $\underline{H}_o$ and the magnetic field caused by the electronic spins is, to a good approximation, in the z direction (Abragam, 1961) and the interaction can be written as

$$-\sum_i \hbar\gamma_i (1+K_{zz}) I_{iz} H_o. \tag{20}$$

It follows that terms E_n through I_n in (15) are zero in this case, and equation (17) obtained for the truncated interaction can therefore be applied. Thus the time-averaged Zeeman interaction is

$$-\sum_i \hbar\gamma_i (1+K) I_{iz} H_o \tag{21}$$

where $K \equiv (1/3)\mathrm{Tr}(\underline{\underline{K}}) = (1/3)(K_1+K_2+K_3)$. For β-tin $K_3 \equiv K_{\parallel}$ and $K_1 = K_2 \equiv K_{\perp}$ because of the $\bar{4}$ axis of symmetry.

In summary, the time-averaged value of $\hbar(E+M+N)$ is

$$\hbar(E+M+N) = \sum_i \hbar\gamma_i (1+K) I_{iz} H_o + \hbar \sum_{i<j} J_{ij} \underline{I}_i \cdot \underline{I}_j \tag{22}$$

when the magic angle condition is satisfied.

II(iii) The Ruderman-Kittel Interaction

The usual method of finding a theoretical expression for the Ruderman-Kittel interaction is to consider $\hbar Q$ as a perturbation of $\hbar(E+F)$ in (1) and to find the second-order correction to the energy levels. The first order correction is responsible for the Knight Shift and will not be discussed here. The second order correction is

$$\Delta E_{o\alpha} = \sum_{n\alpha'} |(0\alpha|\hbar Q|n\alpha')|^2/(E_o+E_\alpha-E_n-E_{\alpha'}) \qquad (23)$$

where $|n\alpha')$ is a product of a many-electron state $|n)$ of energy E_n, and a many-nucleus state $|\alpha')$ of energy $E_{\alpha'}$. The unperturbed state of the electrons and nuclei is $|0\alpha)$. Examination of equation (3) shows that $\hbar Q$ is of the form $\sum_i (H_{en})_i$, that is, it can be written as a sum of terms, each one involving only one nucleus. By expanding $\hbar Q$ in terms of $(H_{en})_i$ one obtains terms of the form

$$|(n\alpha|(H_{en})_i|0\alpha)|^2/(E_o+E_\alpha-E_n-E_{\alpha'}) \qquad (24)$$

which involve only one nucleus. Since we are only interested in interactions involving pairs of nuclei such terms as (24) are omitted and we retain only the cross terms of (23), and thus

$$\Delta E_{o\alpha} = \sum_{i<j} \sum_{n\alpha'} (0\alpha|(H_{en})_i|n\alpha')(n\alpha'|(H_{en})_j|0\alpha)/(E_o+E_\alpha-E_n-E_{\alpha'}). \qquad (25)$$

Because the electronic energy states are essentially continuous and the energy difference between the unperturbed and perturbed electronic states is usually greater than $|E_\alpha-E_{\alpha'}|$, the denominator of (25) is approximated as E_o-E_n. Also, the interaction $(H_{en})_i$ takes the form $\underline{I}_i \cdot \underline{G}_i$, where $\underline{G}_i$ does not involve the nuclear spin operator. Thus

$$\Delta E_{o\alpha} = \sum_{\beta\beta'} \sum_{\alpha'} \sum_{i<j} \{(\alpha|I_{i\beta}|\alpha')(\alpha'|I_{j\beta'}|\alpha) \sum_n (0|G_{i\beta}|n)(n|G_{j\beta'}|0) + \text{c.c.}\}/(E_o-E_n). \qquad (26)$$

We could have obtained $\Delta E_{o\alpha}$ as a first order perturbation contribution if the term $\mathcal{H}_{eff}$ had been added to (1) where

$$\mathcal{H}_{eff} = \sum_{i<j} \sum_{\beta\beta'} I_{i\beta} (J_{ij})_{\beta\beta'} I_{j\beta'} \tag{27}$$

and

$$(J_{ij})_{\beta\beta'} = \sum_n \{(0|G_{i\beta}|n)(n|G_{j\beta'}|0) + c.c.\}/(E_o - E_n). \tag{28}$$

$\mathcal{H}_{eff}$ is equivalent to operator N of (6) if the terms of N which involve only one nucleus are excluded. We shall henceforth assume that the indirect interaction is given by (27).

The right hand side of (28) can be written as (Mahanti and Das, 1968)

$$(J_{ij})_{\beta\beta'} = (J_{ij})^{(1)}_{\beta\beta'} + (J_{ij})^{(2)}_{\beta\beta'} + (J_{ij})^{(3)}_{\beta\beta'} + (J_{ij})^{(4)}_{\beta\beta'} \tag{29}$$

where

$$(J_{ij})^{(1)}_{\beta\beta'} = \sum_n B_n \{(0|G^{cont}_{i\beta}|n)(n|G^{cont}_{j\beta'}|0) + c.c.\}$$

$$(J_{ij})^{(2)}_{\beta\beta'} = \sum_n B_n \{(0|G^{cont}_{i\beta}|n)(n|G^{dip}_{j\beta'}|0) + (0|G^{dip}_{i\beta}|n)(n|G^{cont}_{j\beta'}|0)\}$$

$$(J_{ij})^{(3)}_{\beta\beta'} = \sum_n B_n \{(0|G^{orb}_{i\beta}|n)(n|G^{orb}_{j\beta'}|0) + c.c.\}$$

$$(J_{ij})^{(4)}_{\beta\beta'} = \sum_n B_n \{(0|G^{dip}_{i\beta}|n)(n|G^{dip}_{j\beta'}|0) + c.c.\}$$

and

$$G^{cont}_{i\beta} = a_i \sum_\ell S_{\ell\beta} \delta(\underline{r}_{i\ell} - \underline{R}_i)$$

$$G^{dip}_{i\beta} = b_i \sum_{\ell\beta'} (D_{\ell i})_{\beta\beta'} S_{\ell\beta'}$$

$$G^{orb}_{i\beta} = c_i \sum_\ell L_\beta (\underline{r}_{i\ell})/r^3_{i\ell}$$

$$B_n = (E_o - E_n)^{-1}.$$

Some of the cross terms involving the contact, dipolar and orbital contributions have been excluded from the right hand side of (29) since they are equal to zero when the orbital momentum is quenched (Mahanti and Das, 1968).

If the electron energy surfaces are spherical, the term $(J_{ij})^{(2)}_{\beta\beta'}$ is dipolar in form and contains no diagonal components (Mahanti and Das, 1968). The term $(J_{ij})^{(3)}_{\beta\beta'}$, again assuming spherical energy surfaces, has only diagonal components, while the term $(J_{ij})^{(4)}_{\beta\beta'}$ is composed of two parts, a dipolar part and a diagonal part (Mahanti and Das, 1968). These authors showed that for Rb and Cs, the contributions of $(J_{ij})^{(3)}_{\beta\beta'}$ and $(J_{ij})^{(4)}_{\beta\beta'}$ to the diagonal terms of $\underline{\underline{J}}_{ij}$ are small compared to the contributions of $(J_{ij})^{(1)}_{\beta\beta'}$.

For $(J_{ij})^{(1)}_{\beta\beta'}$ we have

$$(J_{ij})^{(1)}_{\beta\beta'} = a_i a_j \sum_{\underline{nks}} \sum_{\underline{n'k's'}} B\{(\underline{nks}|S_\beta \delta(\underline{r}-\underline{R}_i)|\underline{n'k's'})(\underline{n'k's'}|S_{\beta'}\delta(\underline{r}-\underline{R}_i)|\underline{nks}) + c.c.\} \quad (30)$$

where the sum $\sum_{\underline{nks}}$ in (30) is over occupied Bloch electron states. Also, n represents the band of the Bloch state in the first Brillouin zone, k is the wavevector and s is the electron spin of the electron state. The sum $\sum_{\underline{n'k's'}}$ is over the unoccupied electron states and B is equal to $(E_{\underline{nks}} - E_{\underline{n'k's'}})^{-1}$. This expression has been rewritten as

$$(J_{ij})^{(1)}_{\beta\beta'} = \sum_{ss'nn'kk'} (\underline{nk}|\delta(\underline{r})|\underline{n'k'})(\underline{n'k'}|\delta(\underline{r})|\underline{nk}) e^{-i(\underline{k}-\underline{k}')\cdot\underline{R}_{ij}} (s|S_{\beta'}|s')B(s'|S_\beta|s)$$

by various authors (see for example Slichter, 1963). Here $\underline{R}_{ij} = \underline{R}_i - \underline{R}_j$ and $|\underline{nks}) = |s)|\underline{nk})$. The probability of a state $|\underline{nks})$ being occupied is $f(\underline{nks})$ and of a state $|\underline{nks})$ being unoccupied is $1-f(\underline{nks})$, where f is the Fermi-Dirac distribution function. It follows that

$$(J_{ij})^{(1)}_{\beta\beta'} = \sum_{n\underline{k}} \sum_{n'\underline{k}'} \sum_{ss'} (n\underline{k}|\delta(\underline{r})|n'\underline{k}')(n'\underline{k}'|\delta(\underline{r})|n\underline{k}) e^{-i(\underline{k}-\underline{k}')\cdot\underline{R}_{ij}} \times$$

$$(s|S_\beta|s')(s'|S_{\beta'}|s) B\{1-f(n'\underline{k}'s')\} f(n\underline{k}s) \qquad (31)$$

where the sums $\sum_{n\underline{k}s}$ and $\sum_{n'\underline{k}'s'}$ are now over all states. Because $f(n\underline{k}s)$ is approximately the same for spin up or spin down states, and matrix elements vary slowly with energy, we can replace $f(n\underline{k}s)$ by $f(n\underline{k})$ and B by $(E_{n\underline{k}}-E_{n'\underline{k}'})^{-1}$ (Slichter, 1963). As a result of this approximation, and since

$$\sum_{ss'}(s|S_\beta|s')(s'|S_{\beta'}|s) = \sum_{s}(s|S_\beta S_{\beta'}|s) = \mathrm{Tr}(S_\beta S_{\beta'}) = \delta_{\beta\beta'}/2, \qquad (32)$$

we have

$$(J_{ij})^{(1)}_{\beta\beta} I_{i\beta} I_{j\beta} = (J_{ij})^{(1)} \underline{I}_i \cdot \underline{I}_j$$

$$= -(1/V)^2 \sum_{n\underline{k}} \sum_{n'\underline{k}'} I_{nn'}(\underline{k},\underline{k}') f(n\underline{k})\{1-f(n'\underline{k}')\} e^{i(\underline{k}-\underline{k}')\cdot\underline{R}_{ij}}/(E_{n\underline{k}}-E_{n'\underline{k}'}) \qquad (33)$$

where $I_{nn'}(\underline{k},\underline{k}') = -a_i a_j \frac{V}{2}^2 |\psi_{n\underline{k}}(0)|^2 |\psi_{n'\underline{k}'}(0)|^2$ and $\psi_{n\underline{k}}(\underline{r})$ is the wavefunction of $|n\underline{k})$ in the coordinate representation. Different authors have made various approximations in applying (33). In particular Ruderman and Kittel (1954) assumed that the electron energy surfaces are spherical, and that $I_{nn'}(\underline{k},\underline{k}')$ can be approximated by its value at the Fermi surface. Ruderman and Kittel found that

$$J_{ij} = (2/9\pi)\gamma_e^2\gamma_i\gamma_j\hbar^2 m^* |\psi_{k_f}(0)|^4 F(2k_f|\underline{R}_{ij}|) \qquad (34)$$

where $F(x) = \{x\cos(x) - \sin(x)\}/x^4$ and m^* is the effective electron mass. The form of F(x) is shown in figure 1. A more general expression was obtained by Mahanti and Das (1968), who lifted the restriction that $I_{nn'}(\underline{k},\underline{k}')$ be evaluated at the Fermi surface and that

Figure 1 Graphical Representation of F(x)

The number n shows the position of $x = 2k_f R_{ij}$, where R_{ij} is the distance between nth nearest neighbours.

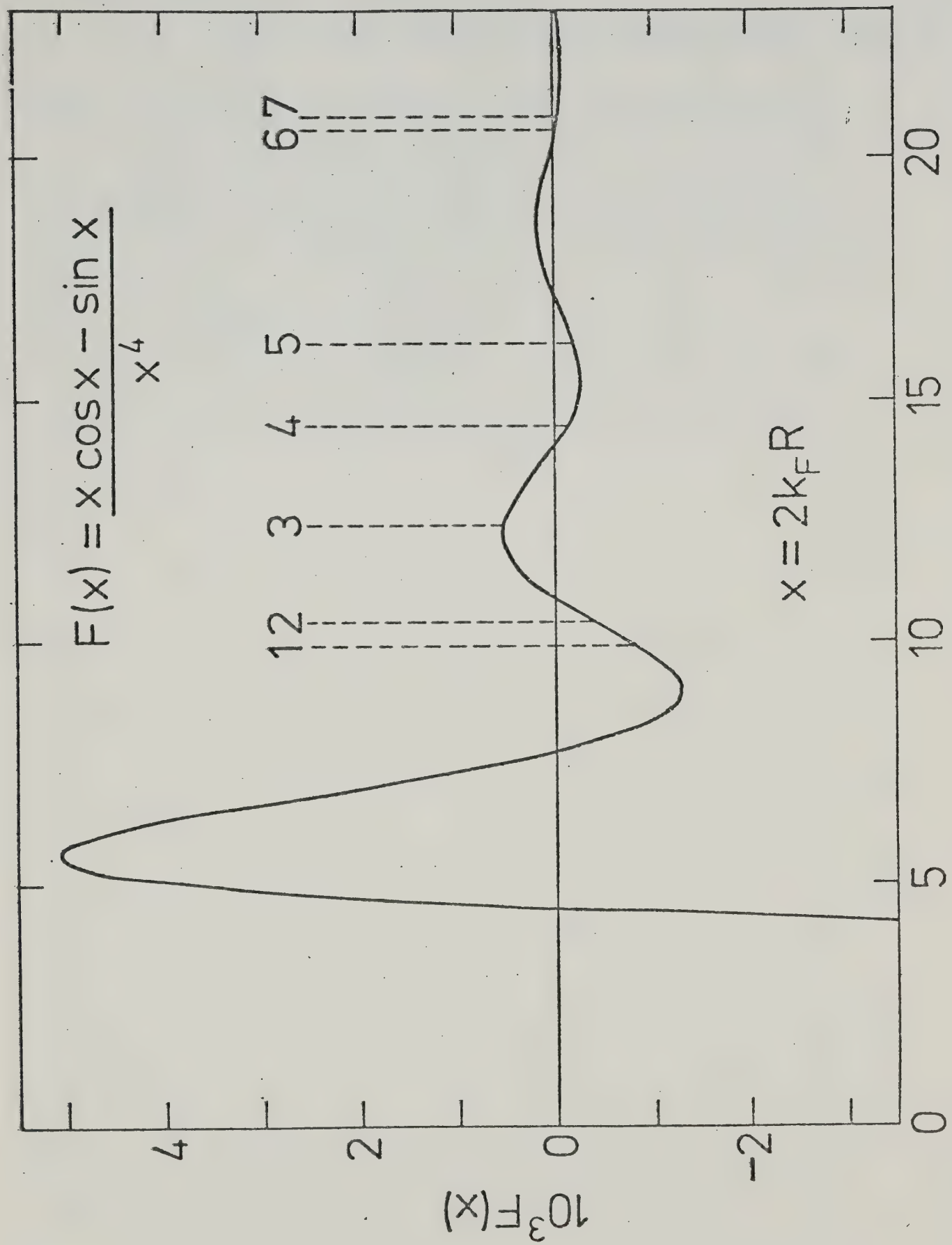
$10^3 F(x)$
4
2
0
-2
0
5
10
15
20
$x = 2k_F R$
$F(x) = \frac{x\cos x - \sin x}{x^4}$
12
3
4
5
67

the bands be parabolic. They obtained

$$J_{ij}^{(1)} = \{c/2(2\pi)^3 R_{ij}^2\} \int_0^{k_f} dk\, m^*(k) k \Phi(n\underline{k}, n\underline{k}'') \sin(2kR_{ij}) \qquad (35)$$

where $c = -(16/3)^2 \pi^2 \gamma_i \gamma_j \gamma_e^2 \hbar^4$ and $\Phi(n\underline{k}, n\underline{k}'') = |\psi_{nk}(0)|^2 |\psi_{nk''}(0)|^2$.

Finally Roth, Zeiger and Kaplan (1966) lifted the restriction of spherical energy surfaces and derived more general expressions for $J_{ij}^{(1)}$. In particular, they found that $J_{ij}^{(1)}$ was proportional to R_{ij}^{-1} for directions perpendicular to two flat regions of the Fermi surface and $J_{ij}^{(1)}$ was proportional to R_{ij}^{-2} for directions perpendicular to the axis of a cylindrical region of the Fermi surface.

II(iv) Theoretical Lineshapes of Configurations of One, Two and Three Magnetic Nuclei

In this thesis we shall be comparing the experimental Sn^{117} resonance in a sample of β-tin which is rapidly rotated at the magic angle, with a theoretical lineshape in which only spin-lattice and Ruderman-Kittel interactions affect the lineshape. Because of the small abundance of magnetic isotopes in natural tin (0.35%, 7.67% and 8.68% for Sn^{115}, Sn^{117} and Sn^{119} respectively (NMR Tables, Varian Associates, 5th edition, 1965)), we synthesize the theoretical lineshape by combining, in appropriate proportions, the lineshapes of nuclei which are interacting with zero, one or two other magnetic nuclei. The probability of finding three or more magnetic nuclei in the vicinity of a particular nucleus is small.

Before proceeding, we shall discuss the application of equation (6) to the particular problem of calculating lineshapes in β-tin. This equation was obtained by assuming that the terms M, N and R' are much less than $1/\tau_c$. For β-tin the Knight Shift is approximately .73% (Smith, 1972) with a result that, for a field of approximately 5 kG, the order of magnitude of M for β-tin is 50 kHz. The magnitude of the Ruderman-Kittel interaction for nearest neighbours is a few kHz. Finally, the magnitude of R' is of the order of 6 kHz since T_1 is approximately 170 microseconds for Sn^{117} (it will be shown in this section that R' is of the order of $1/T_1$). Since $1/\tau_c$ is approximately 10^{11} seconds^{-1}, M, N and R' are much less than $1/\tau_c$.

When non-secular terms are included in equation (6), the effect of the terms $R'_{\alpha\acute{\alpha}\beta\acute{\beta}}$ for which $(\alpha-\acute{\alpha}+\beta-\acute{\beta})\Delta t \gtrsim 1$ can be ignored compared to the effect of terms $R'_{\alpha\acute{\alpha}\beta\acute{\beta}}$ for which

$$(\alpha-\acute{\alpha}+\beta-\acute{\beta})\Delta t \ll 1 \qquad (36)$$

because of the terms $A_{\alpha\acute{\alpha}\beta\acute{\beta}}$ (see equation (11)). As we neglect terms $R'_{\alpha\acute{\alpha}\beta\acute{\beta}}$ which do not satisfy (36) when calculating the lineshapes, we can replace $A_{\alpha\acute{\alpha}\beta\acute{\beta}}$ by the value 1 (the magnitude of $A_{\alpha\acute{\alpha}\beta\acute{\beta}}$ approaches 1 as $(\alpha-\acute{\alpha}+\beta-\acute{\beta})\Delta t$ approaches zero) and regain (6).

The equation can be simplified by considering the high temperature limit and short correlation time approximation, that is when $|E_\alpha - E_{\acute{\alpha}}|/\hbar \ll \tau_c^{-1} < kT/\hbar$, where E_α and $E_{\acute{\alpha}}$ represent eigenvalues of $\hbar(E+M+N)$. We can then replace $R\acute{\sigma} = R'(\sigma-\sigma^T)$ by $R(\sigma-\sigma^T)$ where R is derived from R' by using $k_{q\acute{q}}(\omega) \equiv j_{q\acute{q}}(\omega)e^{\hbar\omega/2kT}$ in place of $j_{q\acute{q}}(\omega)$, the result being that $R_{\alpha\acute{\alpha}\beta\acute{\beta}} = R_{\beta\acute{\beta}\alpha\acute{\alpha}}$. Also we can set $k_{q\acute{q}}(\omega) = k_{q\acute{q}}(0)$ (Redfield, 1957). These approximations can be made since at room temperature (the temperature of the β-tin sample), $kT/\hbar \simeq 4\times10^{13}$ seconds^{-1}, $\tau_c \simeq 10^{-11}$ seconds and $|E_\alpha - E_{\acute{\alpha}}|/\hbar \simeq 10^8$ seconds^{-1}. We make two assumptions about $k_{q\acute{q}}$ which simplify the calculations. The first is that $k_{q\acute{q}}(0) = 0$ unless $q = \acute{q}$. Classically this means that there is no correlation between the random magnetic fields at different nuclear sites and between the various components of the random field at a given nuclear site. This turns out to be a good approximation for β-tin (Winter, 1972). The second assumption is that $k_{qq}(0) = k'$ where k is independent of q. This is a good approximation since McLachlan (1968) found that T_1 for Sn^{119} was essentially orientation independent.

Next we show that the resonance lineshape is unaffected by the operator N which appears in equation (6) provided N commutes with M_x, the x-component of the magnetization operator. The expectation value of M_x, is given by

$$\langle M_x \rangle = \sum_\alpha (\alpha | \sigma M_x | \alpha) \tag{37}$$

and thus

$$\langle \dot{M}_x \rangle = \frac{d\langle M_x \rangle}{dt} = \sum_\alpha (\alpha | \dot{\sigma} M_x | \alpha) \quad . \tag{38}$$

Substituting (6) into (38) we find that

$$\langle \dot{M}_x \rangle = \sum_\alpha (\alpha | [\sigma, E+M+N] M_x | \alpha) \tag{39}$$

As a result, the value of $\langle M_x \rangle$ is not affected by N if $\sum_\alpha (\alpha | [\sigma, N] M_x | \alpha)$ is zero. This is easily shown to be the case if $[M_x, N] = 0$. We have

$$\sum_\alpha (\alpha | \sigma N M_x - N \sigma M_x | \alpha) = \sum_\alpha (\alpha | \sigma M_x N - N \sigma M_x | \alpha) = Tr(\sigma M_x N) - Tr(N \sigma M_x) = 0$$

since the trace is invariant under cyclic permutation of σ, M_x and N.

Finally we include the rf field (linearly polarized in the x direction). If H_{rf} is the rf field interaction, we have for equation (6)

$$\dot{\sigma}_{\alpha\alpha'} = i(E_{\alpha'} - E_\alpha)\sigma_{\alpha\alpha'} + \sum_{\beta\beta} R_{\alpha\alpha'\beta\beta'}(\sigma_{\beta\beta'} - \sigma^T_{\beta\beta'}) + i\{ \sum_{\alpha''} \sigma_{\alpha\alpha''}(\alpha'' | H_{rf} | \alpha') - (\alpha | H_{rf} | \alpha'') \sigma_{\alpha''\alpha} \}. \tag{40}$$

Here E_α is an eigenvalue of the eigenstate $|\alpha)$ for the operator $\hbar(E+M+N)$, and the subscripts refer to the different eigenstates of this operator. From (10) we find

$$R_{\alpha\alpha'\beta\beta'} = (1/2\hbar^2)(2J_{\alpha\beta\alpha'\beta'} - \delta_{\alpha\beta} \Sigma J_{\gamma\alpha'\gamma\beta'} - \delta_{\alpha'\beta'} \Sigma J_{\gamma\beta\gamma\alpha}) \tag{41}$$

where

$$J_{\alpha\beta\alpha'\beta'} = \sum_{jq} 2\hbar^2\gamma_j^2 k'(\alpha|I_{jq}|\beta)(\beta'|I_{jq}|\alpha') \quad . \tag{42}$$

The index j is summed over the nuclei and q takes the values x, y and z. In obtaining (42), we have made use of the approximations involving $k_{qq'}$ ($k_{qq'} = \delta_{qq'}k'$).

In the following subsections A), B), C) and D) we consider the spectrum of nuclei which interact with no unlike nuclei, one unlike and no like nuclei, two unlike and no like nuclei, and one like and one unlike nuclei respectively. For these cases we have $\omega_N = \gamma_N(1+K)H_o$, and W_N is the relaxation rate of the Nth nucleus.

A) No Unlike Nuclei Affecting the Resonance

The lineshape function in this case has been shown previously (Smith, 1972) to be given by

$$\chi(\omega) = 4iZ_X\{i(\omega_X-\omega)-2W_X\}^{-1} \tag{43}$$

where $Z_X = \gamma_X^2\hbar^2\omega_X/32kT$. We note that equation (43) applies whatever the number of like nuclei which are interacting since $J_{ij}\underline{I}_i\cdot\underline{I}_j$, where i and j are any two nuclei of a group of like nuclei, commutes with $M_X = -\sum_\ell \gamma_\ell \hbar I_{\ell x}$, the x-component of the magnetization operator for the group.

B) One Unlike Nucleus (and No Like Nuclei) Affecting the Resonance

For this so-called XA case we generalize the calculation previously made by Smith (1972); we allow for different spin-lattice relaxation rates W_X and W_A for the X and A nuclei.

The four eigenstates are $|++)$, $|+-)$, $|-+)$ and $|--)$ which we number as $|1)$, $|2)$, $|3)$ and $|4)$ respectively. The symbol $|-+)$ represents the state where I_z of the nucleus X (whose spectrum we are determining) is -1/2 and I_z of the unlike nucleus A is +1/2. Using equation (40) we have

$$\dot{\sigma}_{12} = i\omega_{12}\sigma_{12} + i(\sigma_{11}^{T}-\sigma_{22}^{T})H_{21}/\hbar + R_{1212}\sigma_{12} + R_{1234}\sigma_{34} \quad (44)$$

$$\dot{\sigma}_{34} = i\omega_{34}\sigma_{34} + i(\sigma_{33}^{T}-\sigma_{44}^{T})H_{43}/\hbar + R_{3434}\sigma_{34} + R_{3412}\sigma_{12}.$$

Here H_{ij} is $(i|H_{rf}|j)$, while $\omega_{12} = \omega_X - J_{AX}\pi$ and $\omega_{34} = \omega_X + J_{AX}\pi$. Also $\omega_{ij} = (E_j-E_i)/\hbar$ and $H_{ij} = 0$ for $i>j$ except H_{21} or H_{43}. We used $R_{\alpha\beta\alpha\beta}\sigma_{\alpha\beta}$ since $\sigma_{\alpha\beta}^{T}=0$ if $\alpha=\beta$. We have only considered the time derivatives of σ_{12} and σ_{34} since σ_{ij}^{*} is equal to σ_{ji}. Also $\dot{\sigma}_{11}$ and $\dot{\sigma}_{22}$, which are respectively proportional to H_{12}^2 and H_{34}^2, can be ignored for low amplitudes of the rf field. Finally, we do not need to consider σ_{14} and σ_{23} since the rf field does not cause transitions between states $|1)$ and $|4)$ and between $|2)$ and $|3)$. The differences between equations (44) and those of Smith's for this case occur in the relaxation terms, the R's. We recalculate these terms and then alter Smith's results for the lineshape function by taking into account these differences.

It follows from equation (41) that

$$R_{\alpha\beta\alpha\beta} = -\Sigma_j \gamma_j^2 k' \{(\beta|\underline{I}_j^2|\beta)+(\alpha|\underline{I}_j^2|\alpha)\} + 2\Sigma_j \Sigma_q \gamma_j^2 (\alpha|I_{jq}|\alpha)(\beta|I_{jq}|\beta)k'. \quad (45)$$

The first part of the right hand side of (45) is equal to $-(3/2)k'(\gamma_X^2+\gamma_A^2)$ which equals $-(3/2)(W_X+W_A)$ where $k'\gamma_X^2$ is defined as W_X, the spin-lattice relaxation rate for the X nucleus and $k'\gamma_A^2$ is defined as W_A, the spin-lattice relaxation rate of the A nucleus. The second part

of (45) is equal to $(W_A - W_X)/2$ with the result that

$$R_{1212} = R_{3434} = -W_A - 2W_X . \tag{46}$$

By rearranging (41) for the case where α, α', β and β' are all unequal we find

$$R_{\alpha\beta\alpha'\beta'} = \Sigma_j \gamma_j^2 k' \{(\alpha|I_{j+}|\alpha')(\beta'|I_{j-}|\beta) + (\alpha|I_{j-}|\alpha')(\beta'|I_{j+}|\beta)\} \tag{47}$$

where $I_{j+} = I_{jx} + iI_{jy}$ and $I_{j-} = I_{jx} - iI_{jy}$. It follows that

$$R_{1234} = R_{3412} = \gamma_A^2 k' + \gamma_A^2 k' = 2W_A , \tag{48}$$

the lineshape function is given by

$$\chi(\omega) = 2iZ_X(\lambda_{34} + \lambda_{12} - 2W_A)/(\lambda_{12}\lambda_{34} - W_A^2) \tag{49}$$

where $\lambda_{ij} = i(\omega_{ij} - \omega) - W_A - 2W_X$.

C) Two Unlike Nuclei (and No Like Nuclei) Affecting the Resonance

For this case there are three nuclei: the nucleus X (whose spectrum we are calculating), and the two unlike nuclei A and A'. The prime indicates that the two A type nuclei are differently coupled to the X nucleus and the spectrum is called the XAA' spectrum. In his calculations of the XAA' spectrum, Smith (1972) assumed that $W_X = W_A$ and that the A and A' nuclei are not coupled. Since we wish to remove these restrictions it is necessary to recalculate the XAA' spectrum ab initio.

The eigenstates for this case (and case D in which we consider the AA' resonance) are given in table 1(a). In table 1(b) a transition $\alpha \leftrightarrow \alpha'$ is considered to belong to the XAA' spectrum if

Table 1 The Eigenstates and Transition Energies for the $\underline{XAA'}$ and $\underline{AA'X}$ Spectra

Table 1(a) gives the eigenstates and Table 1(b) gives the transition energies in units of h. The symbols D and 2α are defined as $(J_{AA'}^2 + (J_{AX}-J_{A'X})^2/4)^{\frac{1}{2}}/2$ and $\sin^{-1}(J_{AA'}/2D)$ respectively (Pople et al, 1959). Here we have $\nu_{ij} = \omega_{ij}/2\pi$.

$|1) = |+++)$

$|2) = |++-)$

$|3) = \cos\alpha\,|+-+) + \sin\alpha\,|-++)$

$|4) = -\sin\alpha\,|+-+) + \cos\alpha\,|-++)$

$|5) = \sin\alpha\,|+--) + \cos\alpha\,|-+-)$

$|6) = -\cos\alpha\,|+--) + \sin\alpha\,|-+-)$

$|7) = |--+)$

$|8) = |---)$

(a)

LEVELS BETWEEN WHICH THERE IS A TRANSITION	TRANSITION TYPE	TRANSITION ENERGY (IN UNITS OF h)
$8 \longleftrightarrow 6$	AA′	$\nu_{68} = \nu_{AA'} + 1/4\,(-2J_{AA'} - J_{AX} - J_{A'X}) - D$
$7 \longleftrightarrow 4$	AA′	$\nu_{47} = \nu_{AA'} + 1/4\,(-2J_{AA'} + J_{AX} + J_{A'X}) - D$
$5 \longleftrightarrow 2$	AA′	$\nu_{25} = \nu_{AA'} + 1/4\,(2J_{AA'} - J_{AX} - J_{A'X}) - D$
$3 \longleftrightarrow 1$	AA′	$\nu_{13} = \nu_{AA'} + 1/4\,(2J_{AA'} + J_{AX} + J_{A'X}) - D$
$8 \longleftrightarrow 5$	AA′	$\nu_{58} = \nu_{AA'} + 1/4(-2J_{AA'} - J_{AX} - J_{A'X}) + D$
$7 \longleftrightarrow 3$	AA′	$\nu_{37} = \nu_{AA'} + 1/4\,(-2J_{AA'} + J_{AX} + J_{A'X}) + D$
$6 \longleftrightarrow 2$	AA′	$\nu_{26} = \nu_{AA'} + 1/4\,(2J_{AA'} - J_{AX} - J_{A'X}) + D$
$4 \longleftrightarrow 1$	AA′	$\nu_{14} = \nu_{AA'} + 1/4\,(2J_{AA'} + J_{AX} + J_{A'X}) + D$
$8 \longleftrightarrow 7$	X	$\nu_{78} = \nu_{X} - 1/2\,(J_{AX} + J_{A'X})$
$5 \longleftrightarrow 3$	X	$\nu_{35} = \nu_{X}$
$6 \longleftrightarrow 4$	X	$\nu_{46} = \nu_{X}$
$2 \longleftrightarrow 1$	X	$\nu_{12} = \nu_{X} + 1/2\,(J_{AX} + J_{A'X})$
$5 \longleftrightarrow 4$	X	$\nu_{45} = \nu_{X} - 2D$
$6 \longleftrightarrow 3$	X	$\nu_{36} = \nu_{X} + 2D$

(b)

$|\frac{E_\alpha - E_{\alpha'}}{\hbar}|$ is nearer ω_X than ω_A (otherwise the transition belongs to the $\underline{AA'}X$ spectrum). The frequencies ω_X and ω_A are assumed to be far enough apart that the probability of the rf field flipping an A nucleus is negnegligible near ω_X. For the $\underline{X}AA'$ spectrum we need only consider the time derivatives of σ_{12}, σ_{35}, σ_{36}, σ_{45}, σ_{46} and σ_{78}. The time derivatives of the other values of σ_{ij} are not considered because the transitions $i \leftrightarrow j$ are part of the $\underline{AA'}X$ spectrum or for reasons similar to those given in part B. For the $\underline{X}AA'$ spectrum we have

$$\sigma_{\alpha\alpha'} = i\omega_{\alpha\acute{\alpha}}\sigma_{\alpha\acute{\alpha}} + iU_{\alpha\acute{\alpha}} + \Sigma R_{\alpha\acute{\alpha}\beta\acute{\beta}}\sigma_{\beta\acute{\beta}} \qquad (50)$$

where α,α' and β,β' take on values 1,2; 3,5; 3,6; 4,5; 4,6; and 7,8. Also

$$U_{ij} = \hbar^{-1}(\sigma_{ii} - \sigma_{jj}^T)H_{ji} = (2\hbar)^{-1}(\sigma_{ii} - \sigma_{jj}^T)H_{xo}M_{ji}e^{i\omega t}. \qquad (51)$$

Here $M_{ji} = (j|M_x|i)$, where $M_x = -\Sigma_\ell \gamma_\ell \hbar I_{\ell x}$, and H_{xo} is the amplitude of the linearly-polarized rf field of frequency ω. We can approximate U_{ij} as

$$U_{ij} \simeq \omega_X H_{xo} e^{i\omega t}(j|-\Sigma_\ell \gamma_\ell \hbar I_{\ell x}|i)/16kT \qquad (52)$$

since $\sigma_{ii}^T - \sigma_{jj}^T = (e^{-E_i/kT} - e^{-E_j/kT})/(\Sigma_\ell e^{-E_\ell/kT})$

$$\simeq \{(E_j - E_i)/kT\}/(\Sigma_\ell e^{-E_\ell/kT}) \simeq \hbar\omega_X/8kT.$$

It should be noted that $R_{\alpha\acute{\alpha}\beta\acute{\beta}} = R_{\beta\acute{\beta}\alpha\acute{\alpha}}$, and that $R_{1278} = 0$ since $R_{1278} = (1/2\hbar^2)2J_{1728} = (1/\hbar^2)\Sigma_j \Sigma_q 2\hbar^2\gamma_j^2(1|I_{jq}|7)(8|I_{jq}|2)k'$ and $(8|I_{jq}|2) = 0$. For R_{nmnr} where m is not equal to r, we have

$$R_{nmnr} = (2J_{nnmr} - \Sigma_q J_{qmqr})/2\hbar^2 \qquad (53)$$

and

$$\Sigma_q J_{\ell m \ell r} = \Sigma_j \Sigma_q \Sigma_\ell 2\hbar^2\gamma_j^2 k'(\ell|I_{jq}|m)(r|I_{jq}|\ell) \tag{54}$$

$$= \Sigma_j \Sigma_q 2\hbar^2\gamma_j^2 k'(r|I_{jq}^2|m) = \Sigma_j 2\hbar^2\gamma_j^2 3k'(r|m)/4 = 0$$

since the eigenstates are orthogonal. Finally

$$\hbar^{-2}J_{nnmr} = \Sigma_j \Sigma_q 2\gamma_j^2 (n|I_{jq}|n)(r|I_{jq}|m)k' \tag{55}$$

$$= 2k'\{\gamma_A^2(n|I_{Az}|n)(r|I_{Az}|m)+\gamma_A^2(n|I_{Az}|n)(r|I_{Az}|m)\}.$$

Using (54) and (55), we obtain

$$R_{3536} = -R_{3545} = -R_{3646} = -W_A\cos(2\alpha)\sin(2\alpha) \tag{56}$$

where α is defined in table 1.

For R_{mnmn} we have

$$2\hbar^2 R_{mnmn} = 2J_{mmnn} - \Sigma_q(J_{qmqm}+J_{qnqn}) \tag{57}$$

and

$$\Sigma_q(J_{qmqm}+J_{qnqn}) = \Sigma_j \Sigma_q \Sigma_\ell\{2\hbar^2\gamma_j^2(q|I_{j\ell}|m)(m|I_{j\ell}|q)k' + 2\hbar^2\gamma_j^2(q|I_{j\ell}|n)(n|I_{j\ell}|q)k'\}$$

$$= 2\hbar^2\Sigma_j\gamma_j^2 k'\{(n|\underline{I}_j^2|n)+(m|\underline{I}_j^2|m)\} = 3\hbar^2(2W_A+W_X). \tag{58}$$

After determining J_{mmnn} for each R_{mnmn}, we have

$$\begin{aligned} R_{1212} &= R_{7878} = -2W_A-2W_X \\ R_{3535} &= R_{4646} = -3W_A-W_A\cos(2\alpha)-2W_X \\ R_{3636} &= R_{4545} = -3W_A+W_A\cos(2\alpha)-2W_X. \end{aligned} \tag{59}$$

For R_{mnqr} such that all subscripts are different and at least one of the subscripts is not 3, 4, 5 or 6 we have

$$\hbar^2 R_{mnqr} = J_{mqnr} = \Sigma_j \Sigma_\ell 2\gamma_j^2 k'(m|I_{j\ell}|q)(r|I_{j\ell}|n) \tag{60}$$

$$= \Sigma\gamma_j^2 k'\{(m|I_{jj+}|q)(r|I_{j-}|n) + (m|I_{j-}|q)(r|I_{j+}|n)\}.$$

Using (60) we have

$$R_{1235} = R_{1246} = R_{3578} = R_{4678} = W_A \sin(2\alpha)$$
$$R_{1245} = R_{4578} = -R_{1236} = -R_{3678} = W_A \cos(2\alpha). \qquad (61)$$

Finally we need to determine R_{3546} and R_{3645}. In this case

$$\hbar^2 R_{mnqr} = J_{mqnr} = 2k'\gamma_A^2\{(m|I_{Az}|q)(r|I_{Az}|n)+(m|I_{A'z}|n)(r|I_{A'z}|n)\}. \qquad (62)$$

Using (62) we find that $R_{3546} = R_{3645} = W_A \sin^2(2\alpha)$.

Letting $\sigma_{ij} = r_{ij}\exp(i\omega t)$ be the solution, we obtain a set of linear equations, which in matrix form is

$$\underline{\underline{A}}\cdot\underline{r} = iH_{xo}Z_X\underline{P}/\gamma_X h \qquad (63)$$

where $\underline{\underline{A}}$, $\underline{r}$ and $\underline{P}$ are given in table 2(a). To calculate the spectrum we note that

$$\langle M_x\rangle = \Sigma_{ij}\sigma_{ij}(i|M_x|j) = \text{Real}\{-\gamma_X h\underline{r}\ \underline{P}e^{i\omega t}\} \qquad (64)$$

since $-\gamma_X\hbar P_{ij}/2 = (i|M_x|j)$. Since $\langle M_x\rangle$ is equal, by definition, to the real part of $\chi(\omega)H_{xo}e^{i\omega t}$, we have

$$\chi(\omega)H_{xo} = -\gamma_X h\underline{r}\cdot\underline{P}\ . \qquad (65)$$

D) One Unlike Nucleus and One Like Nucleus Affecting the Resonance

The eigenstates for this case are identical with the eigenstates for the $\underline{X}AA'$ spectrum and are given in table 1(a). The transitions and the corresponding frequencies are given in table 1(b). We shall merely quote the result in matrix form since the method is similar to that used to find the $\underline{X}AA'$ spectrum. We find

Table 2 Matrices and Vectors for the $\underline{AA'X}$ and $\underline{XAA'}$ Spectra

The symbols S and C are defined as sin2α and cos2α respectively.

Table 2(a) gives $\underline{A}$, $\underline{P}$ and $\underline{r}$ for the $\underline{XAA'}$ spectrum. Here $\mu_{ij} = i(\omega_{ij}-\omega) - 2W_X - V_{ij}$, where $V_{12} = V_{78} = 2W_A$, $V_{35} = V_{46} = W_A(3+C^2)$ and $V_{36} = V_{45} = W_A(3-C^2)$. Table 1(b) gives $\underline{\underline{A}}$, $\underline{P}$ and $\underline{r}$ for the $\underline{AA'X}$ spectrum. Here $\mu_{ij} = i(\omega_{ij}-\omega) - 3W_A - W_X$; and $p_1 = \sin\alpha - \cos\alpha$ and $p_3 = \sin\alpha + \cos\alpha$.

$$\underline{\underline{A}} = \begin{bmatrix} \mu_{12} & W_A S & -W_A C & W_A C & W_A S & 0 \\ W_A S & \mu_{35} & -W_A CS & W_A CS & W_A S^2 & W_A S \\ -W_A C & -W_A CS & \mu_{36} & W_A S^2 & W_A CS & -W_A C \\ W_A C & W_A CS & W_A S^2 & \mu_{45} & W_A CS & W_A C \\ W_A S & W_A S^2 & W_A CS & W_A CS & \mu_{46} & W_A S \\ 0 & W_A S & -W_A C & W_A C & W_A S & \mu_{78} \end{bmatrix}$$

$$\underline{p}^T = [1, S, -C, C, -S, 1]$$

$$\underline{r}^T = [r_{12}, r_{35}, r_{36}, r_{45}, r_{46}, r_{78}]$$

(a)

$$\underline{\underline{A}} = \begin{bmatrix} \mu_{68} & W_X S & -W_A C & 0 & 0 & -W_X C & -W_A S & 0 \\ W_X S & \mu_{47} & 0 & W_A C & W_X C & 0 & 0 & -W_A S \\ -W_A C & 0 & \mu_{25} & W_X S & W_A S & 0 & 0 & W_X C \\ 0 & W_A C & W_X S & \mu_{13} & 0 & W_A S & -W_X C & 0 \\ 0 & W_X C & W_A S & 0 & \mu_{58} & W_X S & -W_A C & 0 \\ -W_X C & 0 & 0 & W_A S & W_X S & \mu_{37} & 0 & W_A C \\ -W_A S & 0 & 0 & -W_X C & -W_A C & 0 & \mu_{26} & W_X S \\ 0 & -W_A S & W_X C & 0 & 0 & W_A C & W_X S & \mu_{14} \end{bmatrix}$$

$$\underline{r}^T = [r_{68}, r_{47}, r_{25}, r_{13}, r_{58}, r_{37}, r_{26}, r_{14}]$$

$$\underline{p}^T = [p_1, -p_1, p_3, p_3, p_3, p_3, p_1, -p_1]$$

(b)

that

$$\chi(\omega)H_{xo} = -\gamma_A \hbar \underline{r} \cdot \underline{P} \tag{66}$$

where $\underline{r}$ is the solution of the matrix equation

$$\underline{\underline{A}} \cdot \underline{r} = iH_{xo} Z_A \underline{P} / \gamma_A \hbar. \tag{67}$$

Here $\underline{\underline{A}}$ and $\underline{P}$ are given in table 2(b) and $Z_A = \gamma_A^2 \hbar^2 \omega_A / 32kT$.

It should be noted that (66) gives the spectrum for both the A and A′ nuclei. As we require the spectrum for the A nucleus, it is necessary to substitute the vector $\underline{P} = (-a,b,a,b,b,a,b,-a)^T$, where $a = \sin\alpha$ and $b = \cos\alpha$, in place of $\underline{P}$ in (66).

II(v) Theoretical Models of the Ruderman-Kittel Interaction in β-tin

In this section we show how the theoretical Sn^{117} NMR lineshape in β-tin is synthesized. We first consider the spectrum of each Sn^{117} nucleus, taking into account, insofar as possible, the interactions with other magnetic nuclei located in the first, second and third nearest-neighbour shells (since the Ruderman-Kittel interaction is believed to be of moderately short range, it is possible to neglect more distant magnetic nuclei or to treat their effect in a more approximate fashion). We therefore need only consider the more common configurations or small groups in which we find a Sn^{117} nucleus. Because of the complexity of the calculation, we have so far been able to derive expressions only for groups of one, two and three nuclei (apart from the trivial case where there are four or more nuclei which are all identical). This is not a severe limitation since the isotopic abundance of the magnetic nuclei Sn^{115}, Sn^{117} and Sn^{119} is so small (see section II(iv)) that the probability of finding more than two magnetic nuclei in the inner three shells is small (according to Smith (1972), the probability is 19.7%).

We consider three theoretical models for the Ruderman-Kittel interaction in β-tin. For each model we take different relative values of the strength of the first, second and third nearest neighbour interactions. However, before discussing each model individually, we shall describe a slight modification to the notation. By $X\underline{X}A$ we mean

that both the X′ and A nuclei interact with the X nucleus but not with each other. This contrasts with the notation $\underline{XX'}A$ in which there is in general an interaction between all three nuclei. We similarly distinguish between the $A\underline{XA'}$ and the $\underline{XAA'}$ cases.

The first model that we shall consider is the nearest neighbour model. Here, we only consider interactions between nearest neighbour magnetic nuclei (each site has four nearest neighbours). We consider the following basic configurations: $\underline{X}$, $\underline{XA}$, $\underline{XAA'}$, $A\underline{XA'}$, $\underline{XX'}A$ and $X'\underline{X}A$. For this model and the second nearest neighbour model (to be described) there is an interaction between the X′ and A nuclei, but not between the X and A nuclei for the $\underline{XX'}A$ configuration. Similarly there is an interaction between the A and A′ nuclei but not between the X and A′ nuclei for the $\underline{XAA'}$ configuration. Some of the other configurations have resonances which are equivalent to one of the basic configurations (for example, the $\underline{XX'}$ configuration has a resonance which is identical to the $\underline{X}$ configuration, and the $\underline{XAX'}$ configuration has the same spectrum as the $\underline{XA}$ configuration if there is no interaction between the X and X′ nuclei). The probabilities of nuclei having a resonance equivalent to one of the basic configurations' resonances are given in table 3 under the heading 'exact'. For this model, 86.67% of the Sn^{117} nuclei have a resonance equivalent to the resonance of one of the basic configurations. For the remaining 13.33% of the Sn^{117} nuclei, we have approximated their resonance by the resonance of the basic configuration which it most resembles. The probabilities of these approximate resonances are given under the heading 'approx.' and the sum of the exact and approximate probabilities are

SYNTHESIS OF Sn^{117} SPECTRUM (β-TIN)

SPECTRUM	NEAREST-NEIGHBOURS (4) ONLY			SECOND NEAREST-NEIGHBOURS (2) ONLY		
	EXACT	APPROX.	TOTAL	EXACT	APPROX.	TOTAL
$\underline{X}$	0·6173	0·0298	0·6471	0·8139	0·0021	0·8160
$\underline{X}A$	0·1572	0·0040	0·1612	0·1369	0·0000	0·1369
$X'\underline{X}A$	0·0251	0·0386	0·0637	0·0105	0·0033	0·0138
$\underline{X}X'A$	0·0251	0·0153	0·0404	0·0105	0·0010	0·0115
$A\underline{X}A$	0·0193	0·0207	0·0400	0·0068	0·0014	0·0082
$\underline{X}AA'$	0·0227	0·0249	0·0476	0·0113	0·0023	0·0136
TOTALS	0·8667	0·1333	1·0000	0·9899	0·0101	1·0000

Table 3 The Probabilities for the First and Second Nearest Models

given under the heading 'total' in table 3.

The second nearest neighbour model is similar to the nearest neighbour model except that only second nearest neighbour interactions are considered. All other Ruderman-Kittel interactions are assumed to be negligible. As there are only two second nearest neighbour sites for each nuclear site, the probabilities for the configurations listed in table 3 differ from those for the nearest neighbour model.

The third model is the Ruderman-Kittel model. Here we use equation (34) to obtain the relative values of J_{ij} for each nucleus i and j. Using the information given in the caption of figure 2, we obtain relative values of 1.0, 0.478, -0.603 and 0.145 for J_{ij} for first, second, third and fourth nearest neighbour nuclei. We see that the fourth nearest neighbour interaction is relatively small, thereby justifying our decision to treat explicitly only those magnetic nuclei in the inner three shells, which consist of four nearest neighbour, two second nearest neighbour and four third nearest neighbour sites.

The probabilities of occurence of $\underline{X}$, $\underline{X}A$, $\underline{X}AA'$ and $\underline{X}XA$ configurations are given in table V of Smith's thesis and will not be repeated here (in arriving at these probabilities, Smith ignored the Sn^{115} isotope because of its relatively small abundance). However, it should be noted that in 26.7% of the configurations involving three magnetic nuclei, the two magnetic neighbours are either first, second or third nearest neighbours of each other. We have taken such 'cross' interactions into account though they were ignored by Smith.

Finally, we take into account in an approximate fashion the effect of magnetic neighbours outside the inner three shells. The most

Figure 2 Structure of β-tin

The point group symmetry for β-tin is $\bar{4}$ 2 m, with a = 5.831 Å and c = 3.181 Å at room temperature (Pearson, 1967). The numbered nuclei are examples of the nearest neighbours to nucleus A, the number n indicating the nth nearest neighbour. The number of first, second, third and fourth nearest neighbour nuclei are four, two, four and four respectively. Using this structure and the free electron model, we obtain a value of $2k_f = 3.272 \times 10^8 \text{ cm}^{-1}$.

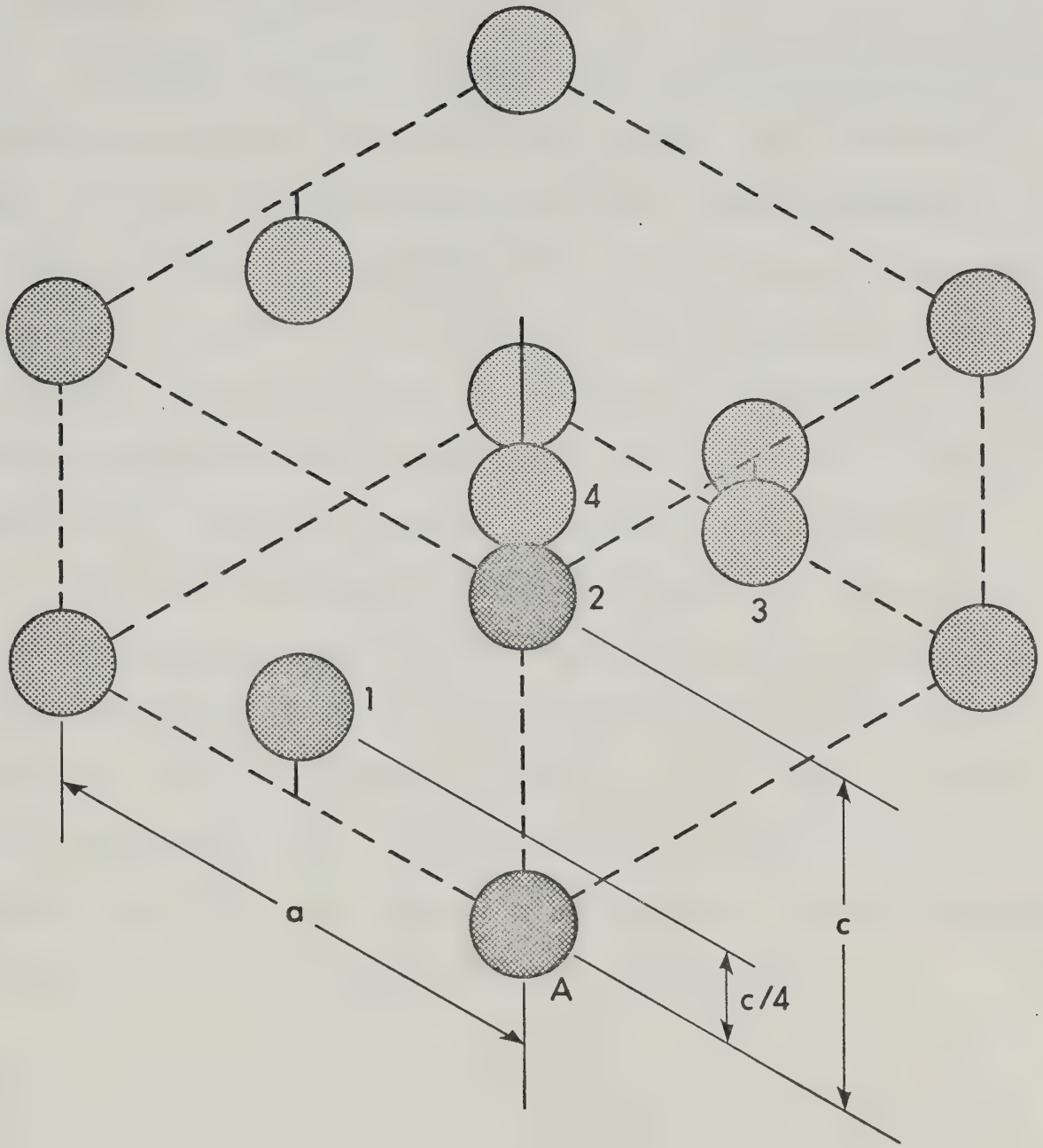
4
2
3
1
a
A
c/4
c

important effect of such nuclei is the broadening produced by the unlike nuclei. However their effect is approximately equivalent to an apparent increase in the relaxation rate of the $\underline{X}$ nucleus. This point is discussed in appendix IV.

It will be seen that we have ignored interactions between the more distant magnetic nuclei and those located in the inner three shells. It can be shown that this is quite a good approximation (D. G. Hughes, private communication). The effect of mutual interactions between nuclei outside the inner three shells are expected to be equivalent to a small reduction in the average spin-lattice relaxation rate of such nuclei. Such effects are taken into account by the introduction of a fitting parameter ξ as described in appendix IV.

The theoretical spectra which are required to synthesize the Sn^{117} lineshape are found using the results of section II(iv). To find the $\underline{X}$ and $\underline{X}A$ lineshapes, we use equations (43) and (49) respectively. The $\underline{X}AA'$ lineshape is given by equation (65) in conjunction with equation (63). The $\underline{X}X'A$ lineshape is given by equation (66) together with (67). The solution of equation(65) is given in appendix II while the solution of (66) is given in appendix III.

III APPARATUS AND EXPERIMENTAL PROCEDURE

In order to study the Ruderman-Kittel interaction, samples of tin were rapidly rotated about an axis inclined at the magic angle to $\underline{H}_o$. While this could be done by spinning the sample about a vertical axis and tilting the magnet until the magic angle condition is satisfied, we chose to spin the sample about an axis inclined to the vertical so that the magnet could be kept horizontal.

The high speed rotation was achieved using an air turbine similar to that pioneered by Beams (1937). In this system air under pressure passes through fine holes or jets drilled at a suitable angle in a conical stator and impinges upon flutings machined into a conical rotor. These jets of air lift the rotor off the stator and start it spinning. The rotor does not fly out of the stator but rides upon a thin cushion of air just above the stator surface, as can be understood by the application of Bernoulli's principle. According to this principle the pressure on the underside of the rotor is related to atmospheric pressure by the relation

$$P_{lower} + \rho v^2/2 = P_{atmos} \qquad (1)$$

where ρ is the density of air and v is the velocity of the air in contact with the underside of the rotor. Since P_{lower} is smaller than P_{atmos}, there is a downward force on the rotor which tends to keep the rotor in the stator. Indeed, this force even enables the rotor to spin upside down.

Since the turbine had to be operated within the rf coils of

the Varian NMR probe, the stator and rotor were made of nylon. Most of the rotors were made out of Delrin (Ertacetyl H) which has better mechanical properties than ordinary nylon (much larger moduli of elasticity and about 20% greater tensile strength). The stator was constructed so that the axis of rotation of the rotor made an angle of 40 degrees to the cylindrical stator support which just fitted within the Varian probe. Because the stator support was perpendicular to $\underline{H}_o$, the axis could make any angle between 50 and 90 degrees with $\underline{H}_o$, merely by rotating the whole stator assembly. The magic angle ($54^o44'$) could therefore be obtained by suitably orientating the stator.

The stator previously described by Smith (1972) was used for the present measurements. However, our rotors differed substantially from those used by Smith, and the design is shown in figure 3. They were hollowed out so as to achieve a maximum sample volume consistent with stable rotation within the Varian probe (inner diameter 1.7 cm). The sample volume of the rotors ranged between 0.23 and 0.25 cm^3 and was 2 or 3 times as large as those used by Smith. Another point should should be made about our design. The center of the plane through x'-x and perpendicular to the axis of symmetry of the rotor, a, is approximately in the same position during rotation. The center of gravity, g, obviously lies along the axis of rotation. As a result, the axis of rotation goes through points g and a to a good approximation. Thus, large perturbations result if the angle between the line g-a and the line a-b is large. This can occur for slight asymmetry of the rotor if g is very close to a. In our design, g was located as far above the x-x' plane as possible. We attribute the improved stability of

Figure 3 The Rotor and Stator

Here a, b, x, x and g are defined in the main body of the thesis; jets of air pass through a from d; e is the stabilizing (relief) jet (Smith, 1972); f gives the position of the walls of the interior of the Varian probe; g′ gives the position of the receiver coils; h and i represent the two parts of the stator which are glued together (Smith, 1972).

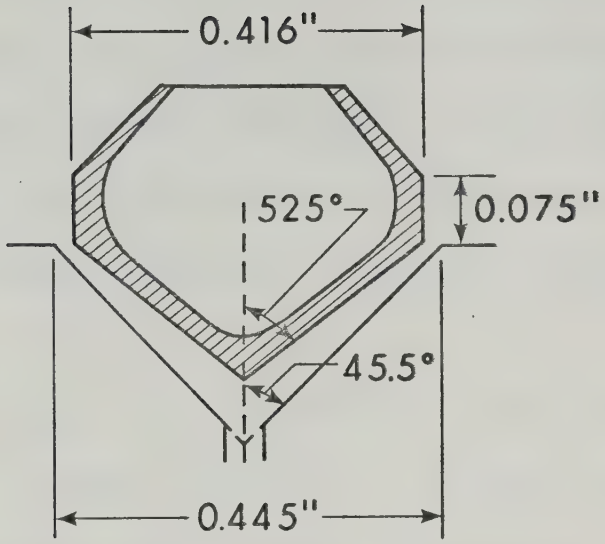
0.416"
0.075"
52.5°
45.5°
0.445"

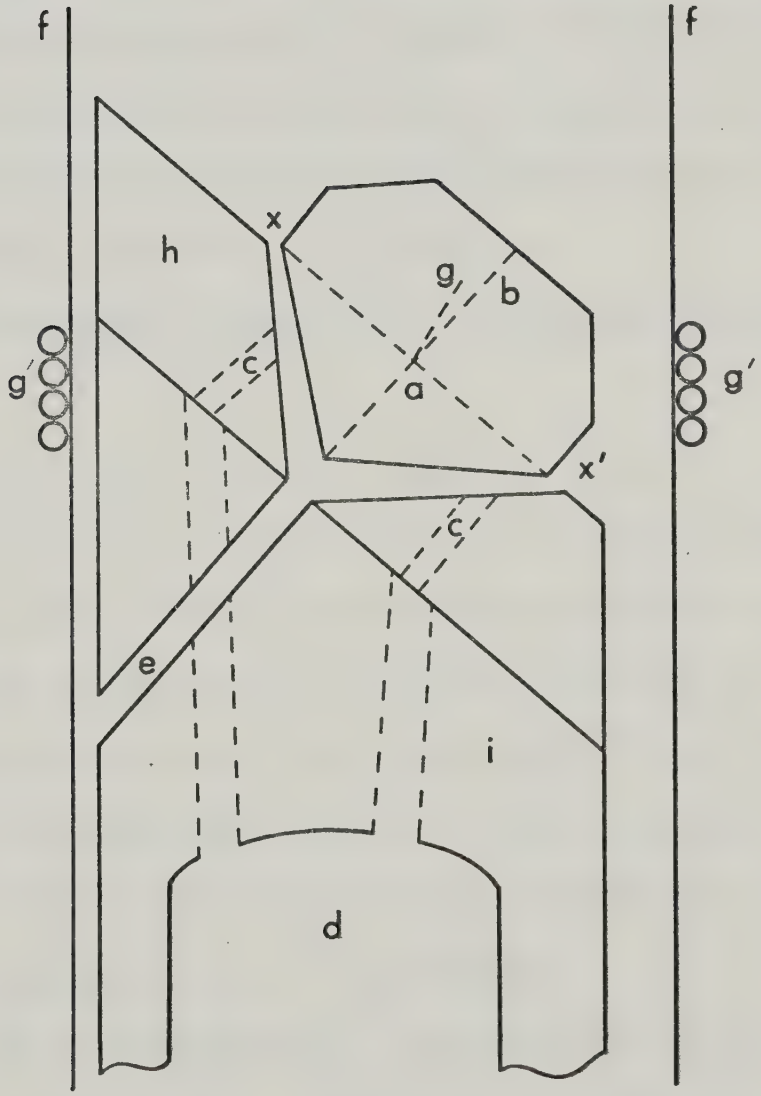
f
f
h
x
g
b
c
a
g'
g'
x'
c
e
i
d

our rotors largely to this modification. We also found that a more stable rotation of the rotors was achieved when the maximum diameter of the rotor was less than the diameter of the top of the conical section of the stator. Both eight and twelve flute rotors were used. However, little consistent difference between the two types was observed.

In order to achieve full penetration of the rf field into the metal, the samples consisted of powder set in epoxy glue. The tin was purchased from Fisher Scientific Company. The purity is believed to be in the range 99.9 to 99.99%. However attempts to confirm this with Fisher Scientific have so far failed. In order to accurately determine the magic angle setting, a small amount of aluminum powder (roughly 10% by volume) was added to the tin powder and the magic angle was obtained using the Al^{27} resonance.

The advantages in using the Al^{27} resonance to find the magic axis are:

(a) The spin-lattice relaxation time, T_1, for Al^{27} is approximately 6.3 milliseconds at room temperature so that the linewidth (defined as the interval between points of maximum and minimum slope of the absorption line) associated with the T_1 broadening is 30 Hz (compared with more than 1 kHz for Sn^{117} and Sn^{119}).

(b) The natural abundance of Al^{27} is 100% which means that the Ruderman-Kittel interaction should not broaden the Al^{27} resonance in pure aluminum (at least in principle).

(c) The peak to peak derivative linewidth in a stationary sample of aluminum is 9.4 kHz (Gutowsky and McGarvey, 1952), where-

as the corresponding linewidth for Sn^{117} and Sn^{119} in pure tin is 3 kHz or more (the precise value depends on the field strength because of the anisotropic Knight Shift).

(d) For equal numbers of nuclei, the NMR signal strength for Al^{27} at constant frequency is more than 8 times as strong as that of Sn^{117}. Moreover only 7.67% of natural tin nuclei are Sn^{117} whereas 100% of aluminum nuclei are Al^{27} (NMR Tables, Varian Associates, 5th edition, 1965).

It should be noted that there is a possibility of a nuclear quadrupole interaction in aluminum on account of the spin number 5/2 of Al^{27} . Lattice defects or strains may give rise to non-zero electric field gradients at the nuclear sites. However, this quadrupole broadening should average out provided the sample is spun sufficiently rapidly.

In making the samples, sufficient epoxy was used to avoid air bubbles in the mixture, since these would seriously unbalance the rotors.

The equipment used to supply the air to the turbine has been described by Smith (1972) and will not be described here. Standard techniques were used to measure the speed of the rotors (Henriot and Huguenard, 1925).

The NMR signals were observed in the absorption mode using a commercial Varian wide-line spectrometer, model VF16B. It was found that the noise output of the spectrometer increased when the rotor was spinning. The excess noise was found to extend over a wide frequency range so that it could not easily be filtered out. Its magni-

tude was found to be proportional to the rf voltage across the transmitter coil, indicating that the source of the problem was a microphonic vibration of the NMR coil system which modulated the coupling between the transmitter and receiver coils. It was found that placing cotton wool near the top of the Varian probe (where the sample was introduced into the probe) reduced the microphonic effect, presumably by damping out the acoustic vibrations. Also, masking tape was placed along the inner walls of the Varian probe (except over the receiver coil) to further reduce microphonics. As a precaution, we reduced the audio bandwidth of the spectrometer immediately following the detector from about 10 kHz to about 500 Hz to prevent overloading due to the large signal present at the frequency of rotation (approximately 5 kHz).

The NMR signals were recorded as the first derivative of the absorption by using a sinusoidal field modulation at 37 Hz in conjunction with lock-in detection. The output of the lock-in detector was fed to a 1024-channel digital signal averager, Fabritek model 1062. A block diagram of the equipment is shown in figure 4.

Synchronization of the magnetic field sweep and the internal sweep of the Fabritek signal averager was achieved by triggering the signal averager with a signal from a photodiode which was turned on by light reflected from a piece of aluminum foil attached to the rotating field-sweep potentiometer of the Varian Fieldial regulator. Repeated sweeps through the resonance made during a 12 hour period were stored in one half of the memory of the signal averager. This procedure enabled us to cancel any slight asymmetry in the signal caused by the

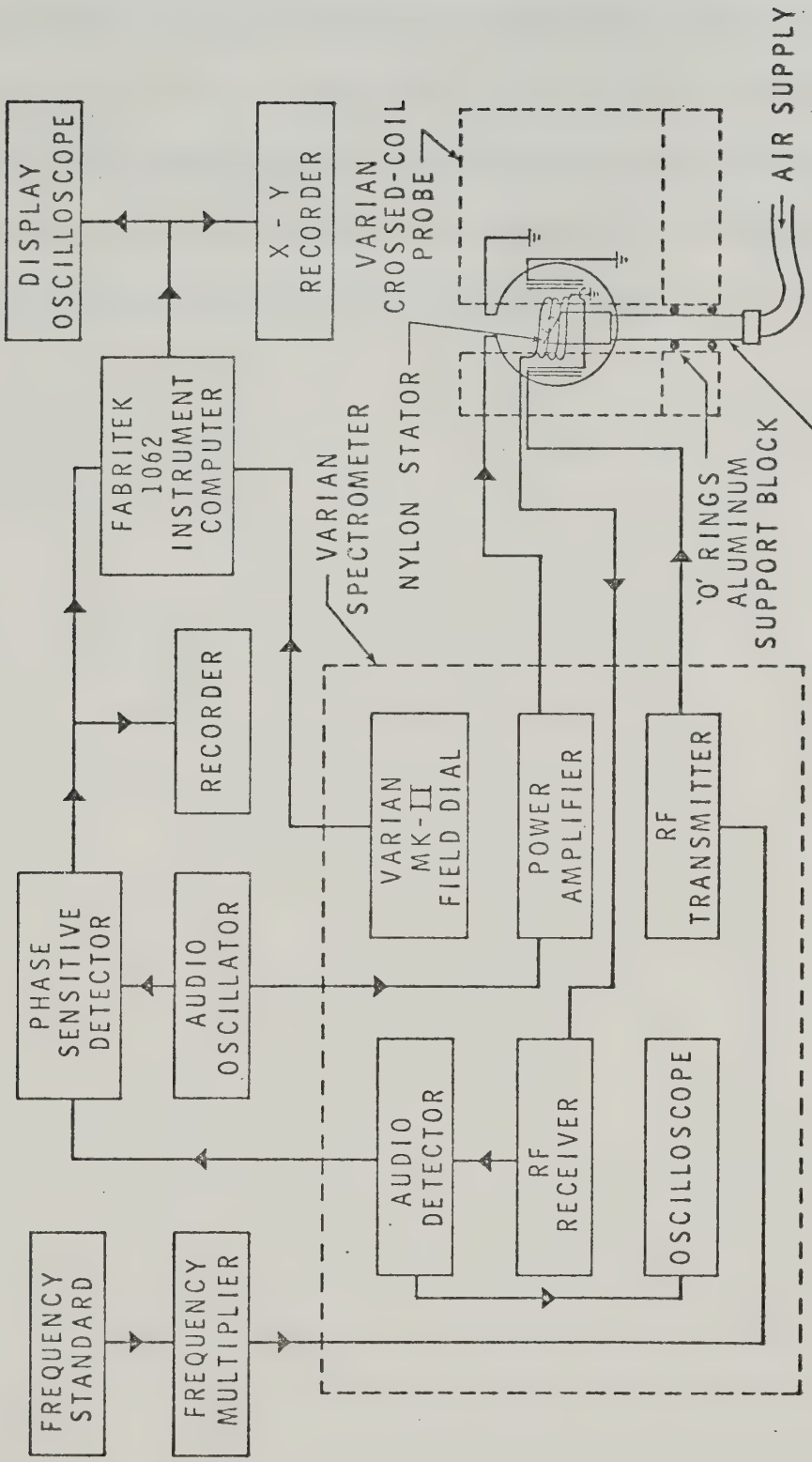

Figure 4 Block Diagram of Apparatus

lock-in detector, by switching the polarity of the signal fed into the signal averager from the lock-in detector after each twelve hour run. The results of each 12 hour run were then transferred (with appropriate polarity) into the other half of the signal averager's memory. After the the entire series of runs was completed, the resonance curve was read out onto an x-y recorder and a theoretical lineshape was fitted to it in the manner described in the next section.

IV RESULTS AND DISCUSSION

IV(i) Experimental Sn^{117} Resonance in β-tin

The derivative of the Sn^{117} NMR absorption signal in a stationary sample of β-tin at room temperature ($22^{o}C$) is shown in figure 5. In obtaining this resonance, H_o was 7000 gauss and the magnitude of the magnetic field modulation was 2.32 gauss. The asymmetry of the resonance is characteristic of the anisotropic Knight Shift in a polycrystalline sample in which the nuclei are located at axially symmetric sites. The rf transmitter voltage was adjusted so that saturation effects (Bloembergen, Purcell and Pound, 1948) were negligible.

The effect of rotating the sample at the magic angle with an angular speed of 5.4 kHz is shown in figure 6. The resonance is the result of summing 25 twelve-hour runs. The resonance is quite symmetric showing that the anisotropic Knight Shift has been averaged out. Rotational sidebands, separated from the main resonance by 5.4 kHz, are clearly visible. In order to obtain a reasonably faithful reproduction of the absorption derivative, the modulation amplitude was reduced to 0.32 gauss in obtaining this resonance. Also, the rf transmitter voltage was reduced to such a level that the loss of peak-to-peak intensity due to saturation amounted to less than 3%. Both these adjustments reduced the signal intensity.

Since we wish to compare the lineshape of the experimental resonance with theory, it is necessary to correct for the residual

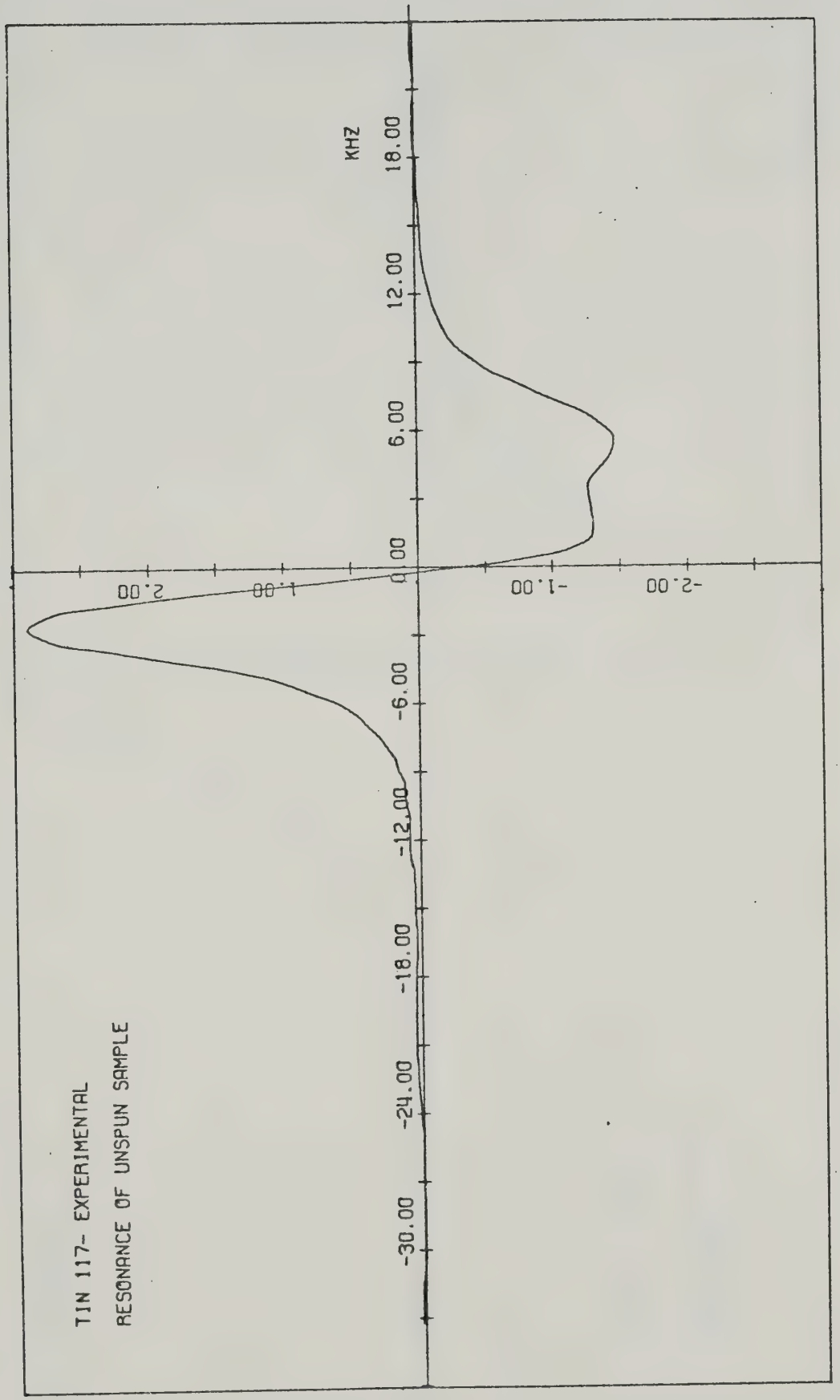

Figure 5-Experimental Resonance (unspun)

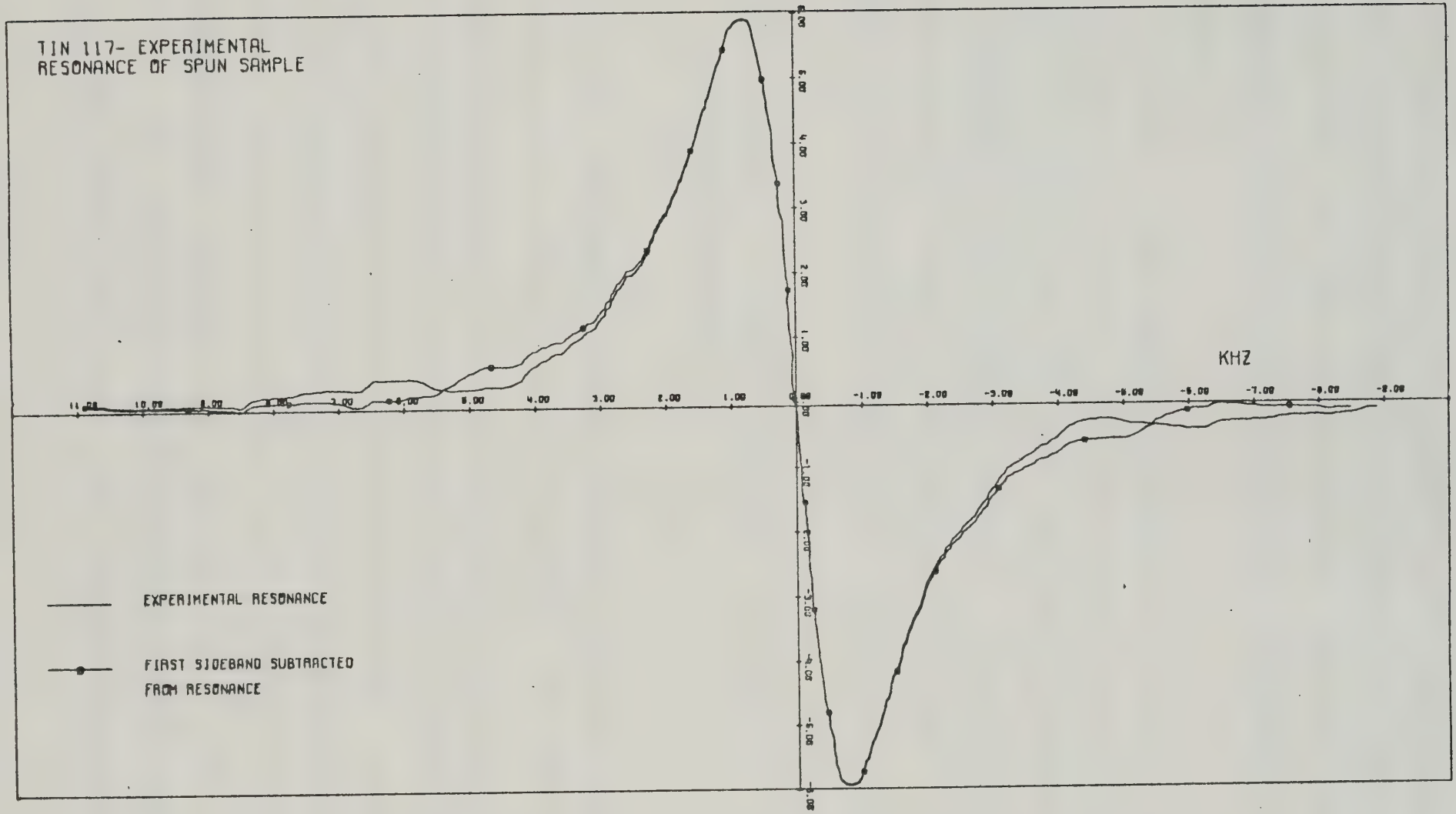

Figure 6 Experimental Resonance (spun at 5.4 kHz)

instrumental distortion caused by the finite modulation amplitude and the rf transmitter voltage. The corrections which are applied to the theoretical rather than the experimental lineshape have been described by Smith (1972). The value of the "saturation" parameter ρ, defined in Appendix IV of Smith's thesis, was .025 for the resonance shown in figure 6.

Finally, the experimental resonance was corrected by subtracting the rotational sidebands. These were assumed to be of the same shape as the main resonance, and their amplitude was estimated by visual examination of the resonance in figure 6. The experimental resonance, corrected by removal of the sidebands, is also shown in this figure. This is the resonance which will be compared with theory.

IV(ii) Procedure For Fitting the Theoretical Lineshape to the Experimental Resonance

The "cross-over" or central frequency, and the baseline of the experimental resonance were first determined. The "cross-over" point can be found quite accurately on account of the steep slope of the absorption derivative near the center, and it was assumed that this point coincides with the center of the theoretical lineshape. Next, the experimental resonance was digitized by measuring the intensity f_i (relative to the previously chosen baseline) at a series of equally spaced frequencies ν_i on either side of the cross-over point. A total of 61 points were taken consisting of the origin (cross-over) and 30 points on each side. Since the interval between

points $\nu_{i+1}-\nu_i$ was 141 Hz, the fitting region extended over 8.46 kHz.

To take account of the different intensity of the theoretical and experimental lineshapes, and to allow for possible error in the baseline determination, the theoretical lineshape intensity at frequencies ν_i was expressed in terms of the normalized theoretical lineshape function $g(\nu)$ in the form

$$h(\nu_i) = \alpha_1 + \alpha_2 g(\nu_i). \qquad (1)$$

The quantities α_1 and α_2 are therefore the baseline correction and normalizing factor respectively.

The fitting was done using the least squares criterion that

$$\chi^2 = \Sigma(f_i - h(\nu_i))^2/\sigma_i^2 \qquad (2)$$

is a minimum with respect to the fitting parameters. The quantity σ_i is the standard deviation of the ith data point as estimated from the signal-to-noise ratio of the experimental resonance.

The normalized theoretical lineshape function $g(\nu)$ is a function of the fitting parameters α_3, α_4, ... α_N, for a total of N-2, while the lineshape function $h(\nu)$ is a function of N parameters. For example, in the nearest and second nearest neighbour models, N is 3 and α_3 is the value of the J coupling between nearest and second nearest neighbours respectively. In the Ruderman-Kittel model, N is 4 since there is an extra fitting parameter α_4 which takes account of interactions with distant nuclei. In this case, α_4 is equivalent to the parameter ξ defined in section II(iv).

For the fitting procedure, we require the values of $\partial g(\nu_i)/\partial \alpha_j$. However, since the calculations of $g(\nu_i)$ in general involve the inver-

sion of an 8×8 matrix (the matrix $\underline{\underline{A}}$ in table 2(b)), this has to be done numerically for each value of i and for each value of α_j, and it is not possible to express $g(\nu)$ as a simple function of the α_j's. We therefore approximate $g(\nu_i)$ in the form of the Taylor expansion

$$g(\nu_i) = A_i + \sum_{j=3}^{N} B_{ij}\delta\alpha_j + \sum_{jk=3}^{N} C_{ijk}\delta\alpha_j\delta\alpha_k \qquad (3)$$

where

$$\alpha_j = \alpha_{jo} + \delta\alpha_j \qquad (4)$$

and α_{jo} is a suitably chosen value of α_j. The coefficients A_i, B_{ij} and C_{ijk} were found for each value of i for the nearest neighbour model (where N = 3) by fitting nine different explicitly calculated theoretical curves to equation (3). The nine theoretical curves corresponded to values of $\alpha_3 = |J_2| = 2.0, 2.25, 2.50, \ldots. 4.0$ kHz, α_{jo} being equal to 3.0 kHz. Since the coefficients are overdetermined, their 'best' value was found using a least squares fit. As a check on the validity of (3) over such an extended range of α_3, the nine theoretical curves were reconstructed using the expansion. They were found to be in excellent agreement with the original explicitly calculated curves. The above procedure was then repeated for the second nearest neighbour model. For the Ruderman-Kittel model where N=4, a total of 18 theoretical curves were used to calculate the coefficients A_i, B_{ij}, and C_{ijk}.

IV(iii) Results

The fits of the experimental resonance of Sn^{117} for the nearest

neighbour model, the second nearest neighbour model and the Ruderman-Kittel model are shown in figures 7, 8 and 9 respectively. For these fits we used a value of T_1 = 169.5 microseconds. This was obtained using the measured value of 155 ± 3 microseconds for Sn^{119} in β-tin at room temperature (295°K) (Dickson, 1969), and using the fact that T_1 is inversely proportional to the square of the gyromagnetic ratio and that $\gamma_{Sn^{119}}/\gamma_{Sn^{117}}$ = 1.046535 ± .000003 (Smith, 1972). The value of σ_i is taken to be .04 intensity units of figure 6 except for the cross-over frequency and the three frequency values on either side of it. For these seven frequency values, σ_i is taken to be .32 intensity units . The fits for the nearest and second nearest neighbour models are poor with χ^2 being equal to 5860 and 12,750 respectively. However, for the Ruderman-Kittel model the fit was good, the value of χ^2 being equal to 127. For this model the value of J, where J is the value of $|J_{i\ell}|$, i and ℓ being a pair of nearest neighbouring Sn^{117} and Sn^{119} nuclei, is 3.04 ± .06 kHz (this implies that J is equal to 2.91 ± .06 kHz for two Sn^{117} nuclei and 3.18 ± .06 kHz for two Sn^{119} nuclei). The error is determined from the fit (Guest, 1961). The value of ξ is .49 ± .05, the error again determined from the fit. We have not taken into account other sources of error; this is done in section IV(iv).

IV(iv) Discussion

It is clear from figures 7 and 8 that the first and second nearest neighbour models are in very poor agreement with experiment.

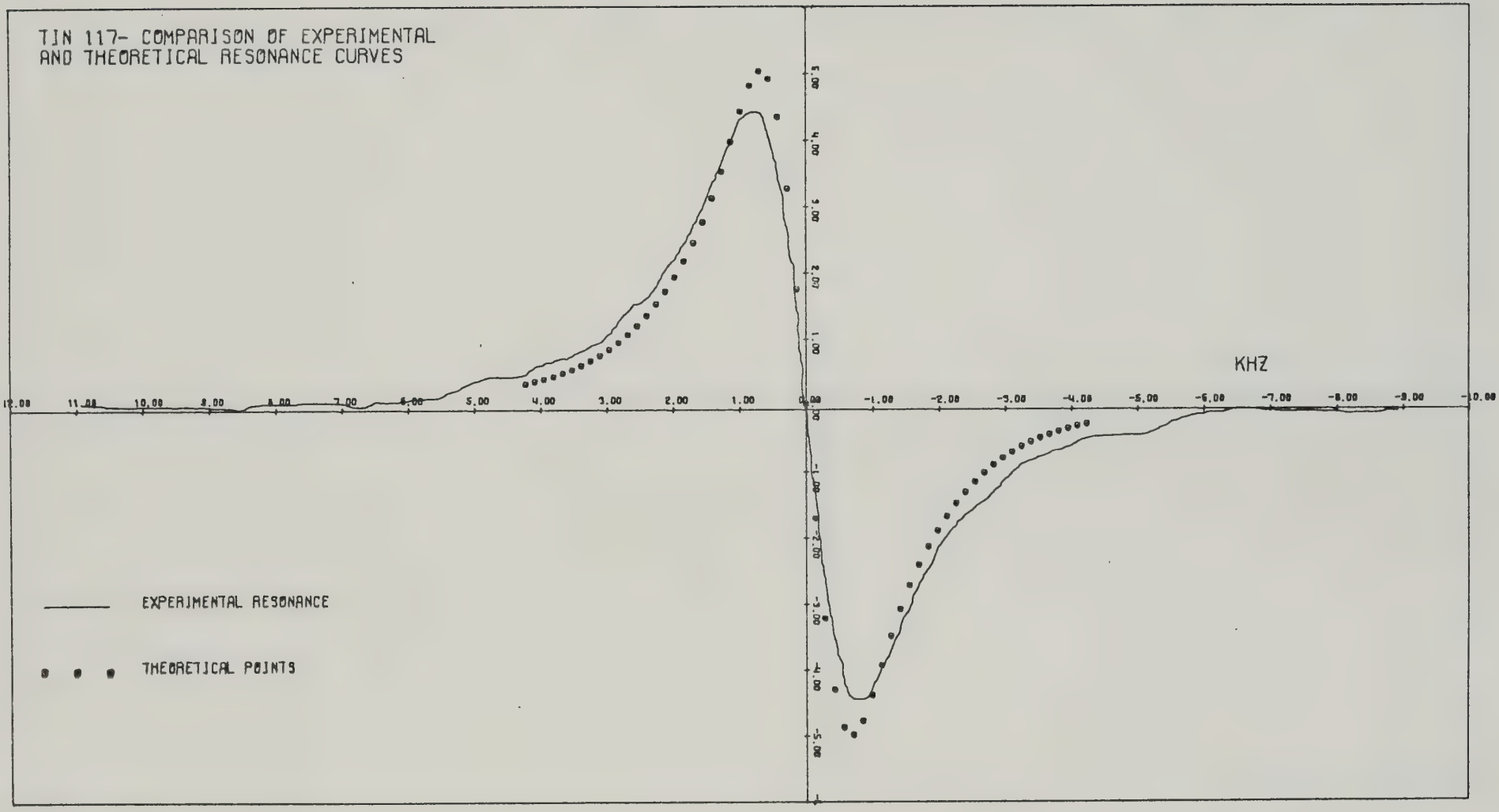

Figure 7 The First Nearest Neighbour Model Fit

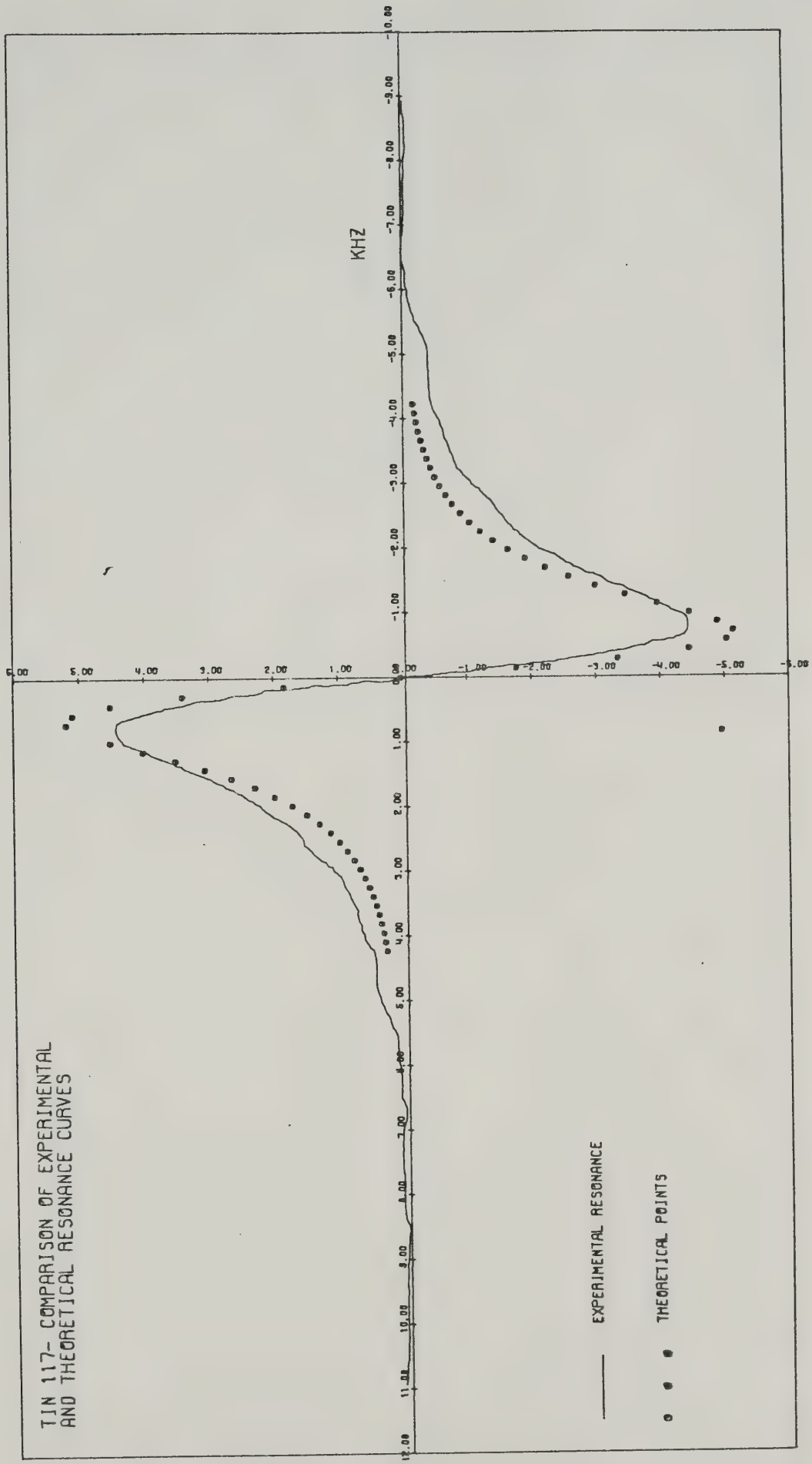

Figure 8 The Second Nearest Neighbour Model Fit

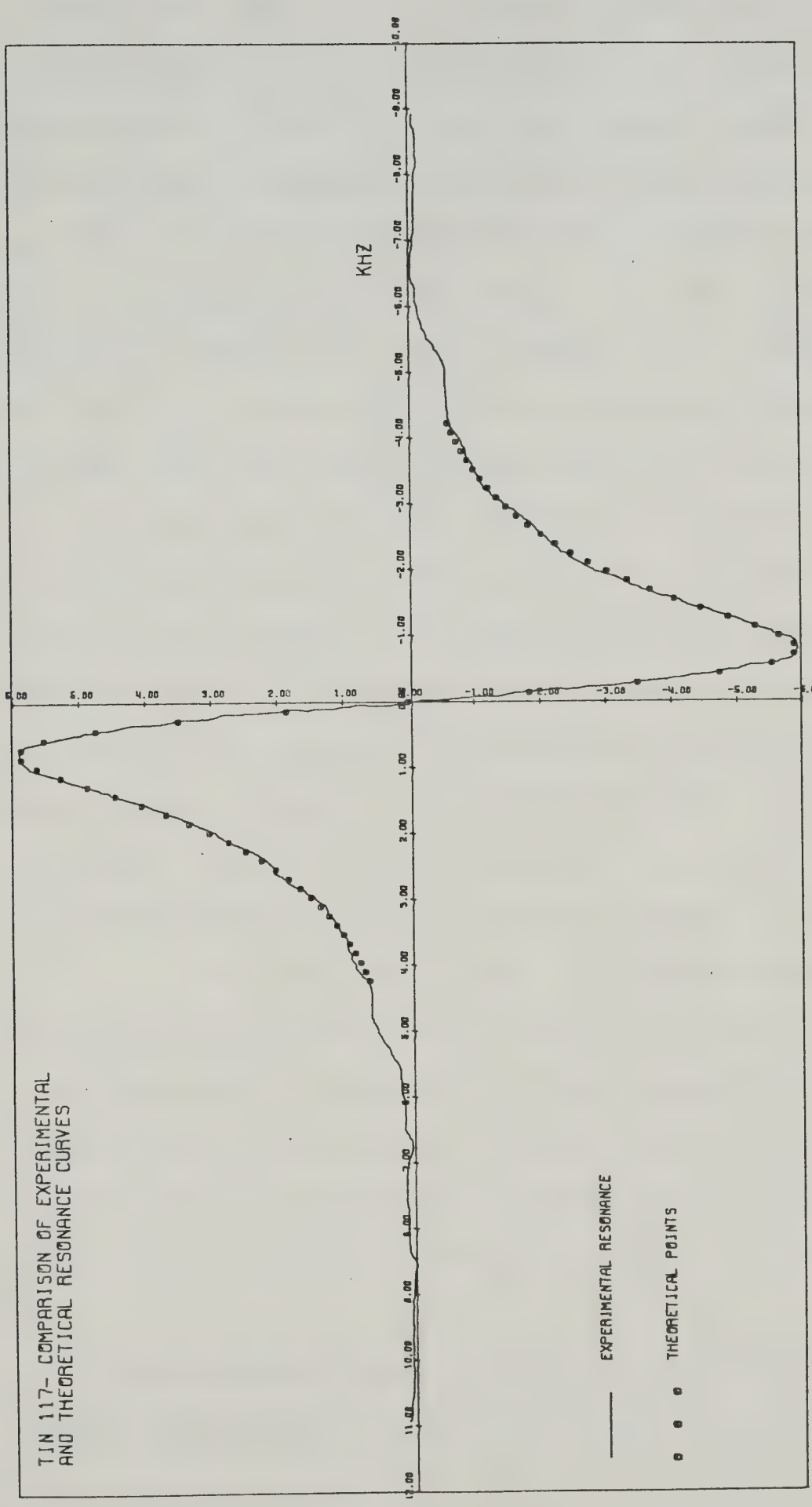

Figure 9 The Ruderman-Kittel Model Fit

It follows that neither the first nearest neighbour nor the second nearest neighbour interaction is dominant in β-tin. It has been suggested (Sharma et al,1969) that the second nearest neighbour interaction could well be dominant, on account of a hole surface in the fourth zone of the Fermi surface with fairly flat faces perpendicular to the [001] direction. According to the results of Roth et al (1966) this should give a strong interaction in the [001] direction, that is, in the direction of the second nearest neighbours. Our results show quite definitely that this is not the case.

It can be seen in figure 9 that the agreement between experiment and the Ruderman-Kittel theoretical model is very good. The 'goodness of fit' parameter χ^2 was found to be 127 as opposed to the 'expected' value of 56. However, such a discrepancy is by no means unreasonable since we estimated the magnitude of the noise by a visual examination of figure 6, an unreliable procedure. On the basis of the results presented in this thesis there is no reason to doubt the validity of the Ruderman-Kittel model as applied to β-tin.

It will be noted that our value of J depends upon the values of T_1 which we have assumed for Sn^{117} and Sn^{119} in β-tin. In order to check this point, we repeated the fitting procedure by assuming a 2% error in the T_1 value as given by Dickson (1969). However, the value of J was found to be changed by only 0.03 kHz, so it is clear that uncertainty in T_1 is not of major importance in our determination of J.

Another possible source of systematic error in our J value arises from the difficulty of estimating the amplitude of the rotation-

al sidebands. Any error in the sideband amplitude will obviously affect the corrected lineshape within the fitting region which extends 4.2 kHz on either side of the cross-over point. We estimate that the error in J arising from this uncertainty is about 0.15 kHz.

Another source of systematic error in our value of J arises from the various approximations made in synthesizing the theoretical lineshape. We estimate this to be about ±.25 kHz. By combining the various errors we estimate our value of J for the interaction between Sn^{117} and Sn^{119} nuclei which are nearest neighbours to be

$$J = 3.04 \pm 0.3 \text{ kHz}.$$

We note that the Ruderman-Kittel fit was really a two-parameter fit, since the parameter ξ representing the effect of distant nuclei was allowed to differ from the value of unity. The fact that ξ was found to be 0.49 ±.05 indicates that the broadening caused by unlike magnetic nuclei outside the inner three shells is significant. We attribute the fact that ξ is less than unity to a combination of the following reasons:

(a) In the derivation of equation (3) in appendix IV, it was assumed that the linewidth contributions due to each distant magnetic nucleus add linearly. However, this is only true if the lineshapes associated with these interactions are Lorentzian (Hughes and MacDonald, 1961) and if they are independent. In actual fact, the lineshapes converge slightly faster than a Lorentzian function (D.G. Hughes, private communication), and one might therefore expect the resulting linewidth to be somewhat smaller than the sum of the individual linewidths, that is, one would expect ξ to be

less than unity.

b) Mutual interactions among the distant magnetic nuclei outside the inner three shells have been neglected. However, mutual spin flips associated with the $J\underline{I}_1 . \underline{I}_2$ interaction will, if the nuclei are of like species, tend to reduce the broadening cause by these nuclei, by a 'motional narrowing' effect. This again would tend to reduce ξ.

(c) No account has been taken of the experimental error in the T_1 value given by Dickson (1969). However, it is intuitively obvious that a 2% error in Dickson's value would have a large effect on ξ.

Apart from the value of 1.89 ± 0.09 kHz found by Smith (1972) for the strength of the Ruderman-Kittel interaction between nearest neaghbours in β-tin, the following values appear in the literature:

2.0 ± 0.5 kHz (McLachlan, 1968)

2.5 kHz (Karimov and Schegolev, 1961)

4.1 ± 0.3 kHz (Alloul and Deltour, 1969).

Also Sharma et al (1969) concluded that the 'exchange narrowing' they observed with a crystal of isotopically pure Sn^{119} was consistent with Alloul and Deltour's value.

A major drawback of the various methods used by McLachlan, Karimov and Schegolev, Alloul and Deltour, and Sharma et al, is their reliance on the measured value of the second moment of the Sn^{119} resonance in natural tin at low temperatures. The difficulty in measuring this second moment is illustrated by the fact that Karimov and Schegolev found that the second moment is 1.2 ± 0.3 $(kHz)^2$ whereas Alloul and Deltour obtained a value of 2.5 ± 0.3 $(kHz)^2$.

In addition, we feel that McLachlan's value of J is unreliable since he assumed that the crystal structure of β-tin is hexagonal close packed and that only the nearest neighbour Ruderman-Kittel interaction was significant.

Karimov and Schegolev, on the other hand, ignored the pseudo-dipolar interaction entirely. This appears to be an important omission since McLachlan found that the pseudo-dipolar interaction was of the same order of magnitude as the dipolar interaction.

Alloul and Deltour's data, obtained using a spin-echo method, is unfortunately by no means easy to interpret. We therefore feel that any discrepancy between their value and ours may well be due to a combination of the approximations made in their theory, and any error in the measured value of the second moment of the Sn^{119} resonance.

Finally, we ask why the value of J obtained by Smith should be so much smaller than our value. We believe that the main cause was the poor signal-to-noise ratio of the resonances obtained by Smith, together with the restricted field sweep used by him (10 gauss compared with 25 gauss in our case). The rotational sidebands are barely visible in Smith's resonances because of the poor signal-to-noise ratio, and they were not corrected for. The 'wings' of the resonance therefore converge more rapidly in the fitting region because of the sidebands, thereby giving the small value of J. Moreover, Smith did not do a two parameter fit as we did. Rather, he had to assume a value for the parameter ξ (proportional to BJ in his notation). The value he assumed turned out to be larger than the one we found. This again would tend to give too small a value of J. Also, in synthe-

sizing the theoretical lineshape Smith made several approximations which we have avoided, though it is difficult to tell whether these would be likely to give too high or too low a value of J.

In order to confirm our value of the strength of the nearest neighbour Ruderman-Kittel interaction, we suggest examining the Sn^{119} resonance in the same way as was done for the Sn^{117} resonance in this thesis. Finally, it should be possible to computationally broaden the Sn^{117} resonance we obtained with the spinning sample, by the anisotropic Knight Shift and direct dipolar broadening, both of which are known. A comparison with the Sn^{117} resonance of the stationary sample would then reveal whether the pseudo-dipolar interaction produces significant broadening in β-tin.

REFERENCES

Abragam A., 1961, The Principles of Nuclear Magnetism, (Oxford: The University Press).

Alloul H. and Deltour R., 1969, Phys. Rev. 183, 414.

Anderson P.W., 1954, J. Phys. Soc. Japan 9, 316.

Andrew E.R., Bradbury A. and Eades R.G., 1958, Nature 182, 1659.

Andrew E.R. and Farnell L.F., 1968, Molec. Phys. 15, 157.

Andrew E.R. and Jenks G.J., 1962, Proc. Phys. Soc. 80, 663.

Andrew E.R. and Newing R.A., 1958, Proc. Phys. Soc. 72, 959.

Beams J.W., 1937, J. Appl. Phys. 8, 795.

Bloch F., Hansen W.W. and Packard M.E.,1946, Phys. Rev. 70, 474.

Bloembergen N., Purcell E.M. and Pound R.V., 1948, Phys. Rev. 73, 679.

Bloembergen N. and Rowland T.J., 1953, Acta Met. 1, 731.

Bloembergen N. and Rowland T.J., 1955, Phys. Rev. 97, 1679.

Davydov A.S., 1966, Quantum Mechanics, (Ann Arbor, Michigan: NEO Press).

Dickson E.M., 1969, Phys. Rev. 184, 294.

Guest P., 1961, Numerical Methods of Curve Fitting, (Cambridge: University Press).

Gutowsky H.S. and McGarvey B.R., 1952, J. Chem. Phys. 20, 1472.

Henriot H. and Huguenard E., 1925, Comptes Rendus 180, 1389.

Hughes D.G. and MacDonald D.K.C., 1961, Proc. Phys. Soc. 78, 75.

Karimov Y.S. and Schegolev I.F., 1961, JETP (English Translation) 13, 908.

Kessemeier H. and Norberg E.R., 1967, Phys. Rev. 155, 321.

Knight W.D., 1949, Phys. Rev. 76, 1259.

Mahanti S.D. and Das T.P., 1968, Phys. Rev. 170, 426.

McLachlan L.A., 1968, Can. J. Phys. 46, 871.

Pake G.E., 1956, Solid State Physics 2, (New York: Academic Press), p. 1.

Pearson W.B., 1967, A Handbook of Lattice Spacings and Structures of Metals and Alloys 2, (Toronto: Pergamon Press), p. 25.

Pople J.A., Schneider W.G. and Bernstein H.J., 1959, High Resolution Nuclear Magnetic Resonance, (Toronto: McGraw-Hill).

Purcell E.M., Torrey H.C. and Pound R.V., 1946, Phys. Rev. 69, 37.

Redfield A.G., 1957, IBM Journal 1, 19.

Roth L.M., Zeiger H.J. and Kaplan T.A., 1966, Phys. Rev. 149, 519.

Ruderman M.A. and Kittel C., 1954, Phys. Rev. 96, 99.

Schwind A.E., 1967, Ann. Physik 7, 22.

Sharma S.N., Williams D.L. and Schone H.E., 1969, Phys Rev. 188, 662.

Slichter C.P., 1963, Principles of Magnetic Resonance, (New York: Harper and Row).

Smith M.R. 1972, Ph.D. Thesis, University of Alberta.

Van Vleck J.H., 1948, Phys. Rev. 74, 1168.

Winter J., 1971, Magnetic Resonance in Metals, (Oxford: Clarendon Press), p. 67.

Appendix I The Time-averaged Values of C_{3n}^2

In this appendix we find the time-averaged values of C_{3n}^2, where C_{3n} is the direction cosine for the nth principal axis of a symmetric, second rank tensor $\underline{\underline{T}}$, with respect to the z axis (the steady magnetic field direction). $\underline{\underline{T}}$ could represent the Knight Shift tensor of β-tin for example. Suppose that the principal axes of $\underline{\underline{T}}$ are x'', y'' and z''. As we want to find the time variation of C_{3n} (in order to obtain the time averaged value of C_{3n}^2), we let x'', y'' and z''' rotate about an axis z' with angular speed Ω. The angle between z and z' is α_3. By determining the vectors x'', y'' and z'' in terms of the fixed laboratory coordinate system xyz, we can evaluate the time variation of C_{3n} (since the above vectors are unit vectors and thus C_{3n} is just the z component of the nth principal axis in the xyz coordinate system). In order to do this we introduce another coordinate system $x'y'z'$ where z' has been previously introduced and the $y'z'$ plane corresponds to the yz plane. The nth principal axis is the vector $(\sin\chi_n \sin(\Omega t+\psi_n), \sin\chi_n \cos(\Omega t+\psi_n), \cos\chi_n)$ in terms of the $x'y'z'$ coordinate system. Here χ_n is the angle between the nth principal axis and z, and ψ_n is the angle which is needed to fix the orientation of the nth principal axis at t = 0. A vector $\underline{A}'$ in the $x'y'z'$ coordinate system is the vector $\underline{A}$ in the xyz coordinate system where $\underline{A} = \underline{\underline{R}}.\underline{A}'$ and

$$\underline{\underline{R}} = \begin{bmatrix} 1 & 0 & 0 \\ 0 & \cos\alpha_3 & -\sin\alpha_3 \\ 0 & \sin\alpha_3 & \cos\alpha_3 \end{bmatrix}$$

Thus the nth principal axis is the vector

$$(\sin\chi_n \sin(\Omega t+\psi_n),\ \cos\alpha_3 \sin\chi_n \cos(\Omega t+\psi_n) - \sin\alpha_3 \cos\chi_n,$$
$$\sin\alpha_3 \sin\chi_n \cos(\Omega t+\psi_n) + \cos\alpha_3 \cos\chi_n)$$

in terms of the xyz coordinate system. Therefore

$$C_{3n} = \sin\alpha_3 \sin\chi_n \cos(\Omega t+\psi_n) + \cos\alpha_3 \cos\chi_n$$

and

$$\overline{C_{3n}^2} = \sin^2\alpha_3 \sin^2\chi_n/2 + \cos^2\alpha_3 \cos^2\chi_n$$

When α_3 satisfied the magic angle condition, $\sin^2\alpha_3 = 2/3$ and $\cos^2\alpha_3 = 1/3$ with the result that $\overline{C_{3n}^2} = 1/3$.

Appendix II: The Absorption Lineshape for the $\underline{XAA'}$ Resonance

In this section we include the expression for the absorption lineshape $\chi''(\omega)$ of the $\underline{XAA'}$ resonance. This was obtained by solving (63) for $\underline{r}$ and then substituting the solution into (65). The $\chi''(\omega)$ was determined from $\chi(\omega)$ by noting that $\chi''(\omega)$ is equal to the imaginary part of $\chi(\omega)$. The solution is

$$\chi''(\omega) = \frac{(\omega_X \gamma_X^2 \hbar^2/16kTW_A)\left[B\{\lambda JL+g(F-2D)-2A-4G\} + c^2\{B(2A+4G+g(2D-F))+ J(EF-2ED-4H-2AK)+2Ab^4\} - 2A(bc)^4\right]}{B\{JC+4A-4gF+8G\}+ c^2\{B(4gF-8G-4A)+J(4AK+8H-4EF)-4Ab^4\}+ 4A(bc)^4}$$

where

$$A = (\lambda g-e)^2 + 4h^2d^2 \qquad G = d^2(\lambda^2+e)$$

$$B = (\lambda g-f)^2 + 4h^2d^2 \qquad H = d^2(\lambda^2+e)(\lambda^2+f)$$

$$C = (\lambda^2-e)^2 + 4\lambda^2d^2 \qquad J = g^2 + d^2$$

$$D = \lambda(\lambda g-e) + 2hd^2 \qquad K = \lambda^2 + d^2$$

$$E = \lambda(\lambda g-f) + 2hd^2 \qquad L = \lambda^2 + d^2 + a^2$$

$$F = (\lambda^2-e)(\lambda g-e) + 4\lambda hd^2 \qquad \lambda = 2(1 + W_X/W_A)$$

$$a = 2\pi(J_{AX}+J_{A'X})/2W_A \qquad e = d^2 - a^2$$

$$b = 2\pi\{4J_{AA'}^2+(J_{AX}-J_{A'X})^2\}^{\frac{1}{2}}/2W_A \qquad f = d^2 - b^2$$

$$c = (J_{AX}-J_{A'X})/\{4J_{AA'}^2+(J_{AX}-J_{A'X})^2\}^{\frac{1}{2}} \qquad g = 2 + \lambda$$

$$d = (\omega_X-\omega)/W_A \qquad h = 1 + \lambda\ .$$

Appendix III: Program to Calculate the AA'X Spectrum

Included in this section is the listing of the subprogram used to find the AA'X spectrum. To find this spectrum, we have to invert the 8×8 matrix given in table 2(b). To do this we have used the cofactor method. In general, this is an inefficient method of solving for the inverse of an 8×8 matrix. However, we have used this method for three reasons. The first is that, as described in the comment statements of the listing, we obtain the intensity of the spectrum as a function of frequency when using this program. This is important because, for this thesis, we need the derivative of the intensity with respect to frequency. This is easily obtainable here since we have the intensity as a function of frequency. If more usual methods of finding an inverse are used, one obtains an intensity value for a certain value of frequency, the result being that one has a discrete set of intensity values. The fact that we obtain the intensity as a function of frequency by one inversion of the matrix means that computer time is saved compared to the more usual methods which would require that the inverse be found for each frequency value. Finally, if certain elements of a matrix are zero, simplifications can be made when finding the inverse by the cofactor method. In our case, 24 out of the 64 elements of the 8×8 matrix are zero.

```
      SUBROUTINE FEED(WW,WWW,IZZZ,A54,N)
C     A DESCRIPTION OF SUBROUTINES USED TO CALCULATE AA'X SPECTRUM.
C
C
C     ALTHOUGH THERE ARE SEVERAL SUBROUTINES USED TO CALCULATE THE
C     AA'X SPECTRUM IT IS ONLY NECESSARY TO CALL THE SUBROUTINE FEED
C     AND ITS TWO ENTRY POINTS(FIRST AND SECOND) BY THE CALLING PROGRAM.
C     ALL OTHER SUBROUTINES ARE CALLED BY FEED.  A DESCRIPTION OF FEED
C     FOLLOWS(A DESCRIPTION OF FIRST AND SECOND FOLLOW THEIR ENTRY
C     STATEMENTS).
C     IT SHOULD BE NOTED THAT FEED IS CALLED ONCE, THEN FIRST IS CAL-
C     LED 36 TIMES, THEN SECOND IS CALLED ONCE FOR EACH AA'X SPECTRUM.
C
C     FEED:
C
C
C                                                              THE VEC-
C     TORS A,ABL,DETT ARE CALCULATED.  WHEN N IS NOT EQUAL TO ZERO, THEN
C     THE SUM OF TERMS A(N+1)*X**N DIVIDED BY THE SUM OF TERMS DETT(M+1)
C     *X**M GIVES THE INTENSITY AT FREQUENCY REAL(B) WHERE, N GOES FROM
C     0 TO 7; M GOES FROM 0 TO 8; AND X=-D-B, D BEING REAL AND B BEING
C     IMAGINARY.  TO OBTAIN THE INDIVIDUAL SPECTRA FOR THE A AND A' NUC-
C     LEI, N IS SET EQUAL TO ZERO.  THEN THE A AND A' SPECTA ARE OB-
C     TAINED BY REPLACING THE VECTOR A IN THE ABOVE SUM BY A AND ABL
C     VECTORS RESPECTIVELY.  THUS BY USING THE VECTORS WITH A CALLING
C     PROGRAM WHICH CALCULATES THE SUMS MENTIONED ABOVE, THE SPECTRA
C     CAN BE EVALUATED.  D SHOULD BE SET TO THE VALUE OF A54 UNLESS
C     THERE IS BROADENING DUE TO NUCLEI NOT IN THE GROUP AA'X SUCH AS IN
C     THE THESIS OF M. SMITH (1972).  FOR THAT THESIS D=BJ*SJI*SJI*.5
C     /WW +A54
C     IZZZ-THIS IS AN INTEGER.  WHEN IZZZ IS NOT EQUAL TO ZERO, THE
C     PRODUCT OF THE MATRIX OF THEORY AND ITS INVERSE IS PRINTED.  THIS
C     PRODUCT MATRIX IS NOT NORMALIZED AND THE FREQUNCY USED IN CALCU-
C     LATING THE MATRIX IS EQUAL TO A54.  IF IZZZ=0,THIS PRODUCT MATRIX
C     IS NOT PRINTED.  THIS IS ONLY USED AS A CHECK OF COMPUTATIONS.
C     A54-THIS IS A REAL NUMBER.  IT IS OF THE ORDER OF THE FREQUENCY
C     FOR WHICH THE RESONANCE INTENSITY IS EQUAL TO .5 TIMES THE MAXI-
C     MUM INTENSITY.
C     N-THIS IS AN INTEGER.  THE FUNCTION OF THIS VARIABLE IS DESCRIBED
C     ABOVE.
C     A DESCRIPTION OF THE PARAMETERS OF THE SUBROUTINE STATEMENT.
C     WW-THIS IS THE TRANSITION RATE FOR THE A OR A' NUCLEI.
C     WWW-THIS IS THE TRANSITION RATE FOR THE X NUCLEUS(WW,WWW ARE IN
C     1/SECONDS)
C     IN ADDITION TO THE ABOVE VARIABLES THE FOLLOWING VARIABLES MUST
C     APPEAR IN A COMMON STATEMENT OF THE CALLING PROGRAM. THE STATEMENT
C     TAKES THE FORM-COMMON/AREA/A(8),DETT(9),ABL(10),XJ1,XJ2,XJ3
C     A-THIS VECTOR IS DESCRIBED ABOVE.  THIS IS A COMPLEX VARIABLE OF
C     DOUBLE PRECISION(COMPLEX*16).
C     DETT-THIS VECTOR IS DESCRIBED ABOVE.  THIS IS A DOUBLE PRECISION
C     COMPLEX VARIABLE(COMPLEX*16)
C     ABL-THIS VECTOR IS DESCRIBED ABOVE.  THIS IS A COMPLEX DOUBLE
C     PRECISION VARIABLE(COMPLEX*16)
C     XJ1,XJ2,XJ3-THESE ARE THE INDIRECT COUPLING CONSTANTS OF THE
C     FIRST,SECOND, AND THIRD NEAREST NEIGHBOURS(IN HZ).
C     THIRTY-SIX RECORDS MUST BE READ FROM LOGICAL UNIT 2.  THE FOL-
C     LOWING 36 CARDS DISPLAY THE CONTENTS OF THE 36 RECORDS, EACH RE-
```

```
      C     CORD CONSISTING OF 23 LETTERS.
      C     BCDEFGHJKPILKLMINJIOOOO                                  CARD1
      C     ICDEFGHJKPILKLMINJINMPO                                  CARD2
      C     NBDEFGHILKJKPLMINJIIMPO                                  CARD3
      C     MGDEBCHLIJMNIJIKLPKPINO                                  CARD4
      C     PFEDBCHNMIILJKLJIPKMINO                                  CARD5
      C     BCEHFGOKPILKNINJIMPJILM                                  CARD6
      C     BCDEFGOJKIILNLMINMPPKJI                                  CARD7
      C     HACFDEGKJINMPILLIMNOOOO                                  CARD8
      C     AHFGDEOMPIJIPLIMNJKNKIL                                  CARD9
      C     KHFGADCINLJIKMLPMNIPIJO                                  CARD10
      C     AHCFDEONMIKJPILLIJKPIMN                                  CARD11
      C     PEFCADGJKIILNMLNIPMKIJO                                  CARD12
      C     AHGBDEFPIMIPJMNJKLIOOOO                                  CARD13
      C     IHBFAEGJLMPJIIKMIPNKNLO                                  CARD14
      C     LHFGDABINKJIPLMMPJIKINO                                  CARD15
      C     AHGBDEOPINIPKMNJKILMJLI                                  CARD16
      C     KEBFDAGPJIKINJILMMPLINO                                  CARD17
      C     BCEAFGHKIPLNKINMPJIOOOO                                  CARD18
      C     BCAHFGOIPJNKIMPJILMKLIN                                  CARD19
      C     LGAEBCHMIJPNIINKLPKMJIO                                  CARD20
      C     MFAEBCHPNIMIJINKLPKLJIO                                  CARD21
      C     JAFGEHCLMIMPNIJNILKIKPO                                  CARD22
      C     BCDAFGHJIPINKLMMPJIOOOO                                  CARD23
      C     IGADBCHMLJPMIINJIPKNKLO                                  CARD24
      C     NFADBCHPMIMLJINJIPKIKLO                                  CARD25
      C     BCADFGOIJKNILMPLMINPKJI                                  CARD26
      C     AHBCDEGINPPKIJKILMNOOOO                                  CARD27
      C     ADBCEHOINMJILKPLKIJPMNI                                  CARD28
      C     AHBCDEFINMPKJJKILLIOOOO                                  CARD29
      C     IECBADFKPJLKINIIJMLNPMO                                  CARD30
      C     JDGBAECIPKMJIPNIKNLLMIC                                  CARD31
      C     CBADFGENILIJKMPLMINOOOO                                  CARD32
      C     BCHDFGOPJIKINJILMMPKLIN                                  CARD33
      C     AHCGDEONPIKIPILMNJKMJLI                                  CARD34
      C     AHBFDEOIMNPJKJKLIILPIMN                                  CARD35
      C     BCAEFGOIKJNLIMPINLMPKJI                                  CARD36
      C     THE ABOVE 36 RECORDS MUST BE READ EACH TIME VECTORS ARE REQUIRED
      C     FOR AN AA'X SPECTRUM.  AFTER THE READING OF THE 36 RECORDS,LOGICAL
      C     UNIT 2 IS REWOUND BY SUBROUTINE.
      C
      C
            COMPLEX*16 DETT,A,ABL
            COMPLEX*16 ALL(10),AXX,XRET(36,7),Z4,DDX,X2(40,8),F1(8,8),DX,DET
           $ (7,8),RX,Z(7),TT(8)
            REAL HACOS,HASIN
            COMPLEX XFAT
            COMPLEX CMPLX
            DIMENSION II(23),III(23)
            REAL*8 AL(8,8),STORE(36,16),X4(16)
            COMMON Z,X4
            COMMON TT
            COMMON XGAM1,XGAM2,XGAM3,XGAM4,XGAM5,XGAM6
            COMMON/AREA2/F1,XRET,STORE
            COMMON/AREA/A(8),DETT(9),ABL(10), XJ1,XJ2,XJ3
            DATA III/'A','B','C','D','E','F','G','H','I','J','K','L','M','N',
           $'P','Q','R','S','T','U','V','W','O'/
            DO 311 JKK=1,8
        311 ALL(JKK)=0.
            R9=-3.*WW-WWW
```

```
      PI=3.141593
      SPI=2.*PI
      XJ1=SPI*XJ1
      XJ2=SPI*XJ2
      XJ3=SPI*XJ3
      DD=.5*SQRT(.25*(XJ2-XJ3)**2+XJ1**2)
      RCOS=1.
      RSIN=0.
      IF(DD.NE.0.)RSIN=.5*XJ1/DD
      IF(DD.NE.0.)RCOS=.25*(XJ2-XJ3)/DD
      R1=(-2.*XJ1-XJ2-XJ3)/4.-DD
      R2=(-2.*XJ1+XJ2+XJ3)/4.-DD
      R3=(2.*XJ1-XJ2-XJ3)/4.-DD
      R4=(2.*XJ1+XJ2+XJ3)/4.-DD
      R5=R1+2.*DD
      R6=R2+2.*DD
      R7=R3+2.*DD
      R8=R4+2.*DD
      R1=R1+A54
      R2=R2+A54
      R3=R3+A54
      R4=R4+A54
      R5=R5+A54
      R6=R6+A54
      R7=R7+A54
      R8=R8+A54
      IF(N.NE.0)GO TO 309
      HACOS=SQRT(.5*(RCOS+1.))
      HASIN=SQRT(.5*(1.-RCOS))
      IF(RSIN.GT.0.)GO TO 308
      HACOS=-HACOS
  308 IF(HACOS.EQ.HASIN)GO TO 309
      IF(HACOS.EQ.-HASIN)GO TO 309
      DUM1=HACOS+HASIN
      DUM2=HACOS-HASIN
      ALL(1)=CMPLX(HACOS/DUM2,0.)
      ALL(2)=CMPLX(-HASIN/DUM2,0.)
      ALL(3)=CMPLX(HACOS/DUM1,0.)
      ALL(4)=CMPLX(HASIN/DUM1,0.)
      ALL(5)=ALL(4)
      ALL(6)=ALL(3)
      ALL(7)=ALL(2)
      ALL(8)=ALL(1)
  309 CONTINUE
      I11=0
      DO 1 I1=1,36
      I11=I11+1
      READ(2,1000)(II(L1),L1=1,23)
      DO 1 M1=1,23
      M2=M1-7
      IF(M1.EQ.1)M2=M1
      IF(M1.EQ.1)XRET(I11,1)=(0.,0.)
      IF(II(M1).EQ.III(1 ))XRET(I11,M1)=CMPLX(R9,R1)
      IF(II(M1).EQ.III( 2))XRET(I11,M1)=CMPLX(R9,R2)
      IF(II(M1).EQ.III( 3))XRET(I11,M1)=CMPLX(R9,R3)
      IF(II(M1).EQ.III( 4))XRET(I11,M1)=CMPLX(R9,R4)
      IF(II(M1).EQ.III( 5))XRET(I11,M1)=CMPLX(R9,R5)
      IF(II(M1).EQ.III( 6))XRET(I11,M1)=CMPLX(R9,R6)
      IF(II(M1).EQ.III( 7))XRET(I11,M1)=CMPLX(R9,R7)
      IF(II(M1).EQ.III( 8))XRET(I11,M1)=CMPLX(R9,R8)
```

```
182           IF(II(M1).EQ.III( 9))STORE(I11,M2)=WWW*RSIN
183           IF(II(M1).EQ.III(10))STORE(I11,M2)=WW*RCOS
184           IF(II(M1).EQ.III(11))STORE(I11,M2)=WWW*RCOS
185           IF(II(M1).EQ.III(12))STORE(I11,M2)=WW*RSIN
186           IF(II(M1).EQ.III(13))STORE(I11,M2)=-WWW*RCOS
187           IF(II(M1).EQ.III(14))STORE(I11,M2)=-WW*RCOS
188           IF(II(M1).EQ.III(15))STORE(I11,M2)=-WW*RSIN
189           IF(M1.NE.1)GO TO 25
190           CC=AIMAG(XRET(I11,1))
191           XYY=STORE(I11,1)
192           IF(CC.EQ.0.) XRET(I11,1)=CMPLX(      XYY.   ,0.)
193        25 CONTINUE
194           IF(M1.GT.15)GO TO 12
195           IF(II(M1).EQ.III(23))XRET(I11,M1)=(0.,0.)
196           GO TO 1
197        12 IF(II(M1).EQ.III(23))STORE(I11,M2)=0.
198         1 CONTINUE
199           JK=0
200           KKK=2
201      1000 FORMAT(23(A1))
202           CALL REWIND(2)
203           RETURN
204           ENTRY FIRST(I11)
205     C
206     C
207     C
208     C     FIRST:
209     C
210     C
211     C     I11-THIS IS AN INTEGER.  WHEN FIRST IS CALLED FOR THE FIRST TIME
212     C     FOR EACH AA'X SPECTRUM, I11=1.  EACH ADDITIONAL TIME I11 IS INCRE-
213     C     MENTED BY 1.  THUS ON THE LAST CALL TO FIRST FOR EACH AA'X
214     C     SPECTRUM I11=36.
215           Z4=(1.,0.)
216           RX=(1.,0.)
217           JK=0
218           DO 3 M2=1,7
219           Z(M2)=XRET(I11,M2)
220         3 CONTINUE
221           DO 14 M2=1,16
222        14 X4(M2)=STORE(I11,M2)
223           CC=AIMAG(XRET(I11,1))
224           IF(CC.EQ.0.)GO TO 10
225           CC=AIMAG(XRET(I11,7))
226           IF(CC.EQ.0.)GO TO 11
227           JK=1
228           CALL ZERO(JK)
229           DO 31 I=1,8
230        31 TT(I)=TT(I)*(-1.,0.)
231           GO TO 6
232        10 CALL NZERO(KKK)
233           GO TO 6
234        11 CALL ZERO(JK)
235           GO TO 6
236         6 CONTINUE
237           DO 27 I=1,8
238        27 X2(I11,I)=TT(I)
239           Z4=TT(1)
240           IF(I11.GT.5)GO TO 4
241           DO 20 I=1,8
```

```
242         20 DET(I11,I)=TT(I)
243          4 IF(I11.NE.8)GO TO 5
244            DO 15 I=1,8
245            RX=(0.,0.)
246            IF(I.NE.1)RX=DET(1,I-1)
247            DETT(I)=DET(1,I)*XRET(8,2)+RX
248            DO 15 M2=2,5
249            M1=M2+1
250         15 DETT(I)=DET(M2,I)*STORE(8,M1)+DETT(I)
251            DETT(9)=DET(1,8)
252          5 CONTINUE
253            RETURN
254            ENTRY SECOND
255            DO 22 I=1,8
256            F1(1,1)=X2(1 ,I)
257            F1(1,2)=X2(2 ,I)
258            F1(1,3)=X2(3,I)
259            F1(1,4)=X2(6,I)
260            F1(1,6)=X2(4,I)
261            F1(1,7)=X2(5,I)
262            F1(1,8)=X2(7,I)
263            F1(2,2)=X2(8,I)
264            F1(2,3)=X2(9,I)
265            F1(2,5)=X2(10,I)
266            F1(2,7)=X2(11,I)
267            F1(2,8)=X2(12,I)
268            F1(3,3)=X2(13,I)
269            F1(3,4)=X2(14,I)
270            F1(3,5)=X2(15,I)
271            F1(3,6)=X2(16,I)
272            F1(3,8)=X2(17,I)
273            F1(4,4)=X2(18,I)
274            F1(4,5)=X2(19,I)
275            F1(4,6)=X2(20,I)
276            F1(4,7)=X2(21,I)
277            F1(2,4)=X2(22,I)
278            F1(5,5)=X2(23,I)
279            F1(5,6)=X2(24,I)
280            F1(5,7)=X2(25,I)
281            F1(5,8)=X2(26,I)
282            F1(6,6)=X2(27,I)
283            F1(6,7)=X2(28,I)
284            F1(7,7)=X2(29,I)
285            F1(7,8)=X2(30,I)
286            F1(6,8)=X2(31,I)
287            F1(8,8)=X2(32,I)
288            F1(1,5)=X2(33,I)
289            F1(2,6)=X2(34,I)
290            F1(3,7)=X2(35,I)
291            F1(4,8)=X2(36,I)
292            DO 13 N2=1,8
293            DO 13 N1=1,8
294         13 F1(N1,N2)=F1(N2,N1)
295            IF(I.NE.1)GO TO 21
296            CALL CHECK(IZZZ)
297            D1=1.-RSIN
298            D2=1.+RSIN
299            D3=RCOS
300            AL(1,1)=D1
301            AL(1,2)=-D1
```

```
      DO 300 J1=3,6
  300 AL(1,J1)=-D3
      AL(1,7)=D1
      AL(1,8)=-D1
      AL(3,1)=-D3
      AL(3,2)=D3
      DO 301 J1=3,6
  301 AL(3,J1)=D2
      AL(3,7)=-D3
      AL(3,8)=D3
      DO 304 J2=4,6
      DO 304 J1=1,8
  304 AL(J2,J1)=AL(3,J1)
      DO 302 J1=1,8
      D4=AL(1,J1)
      AL(7,J1)=D4
      AL(8,J1)=-D4
      AL(2,J1)=-D4
  302 CONTINUE
   21 CONTINUE
      A(I)=(0.,0.)
      ABL(I)=(0.,0.)
      DO 303 J1=1,8
      AXX=ALL(J1)
      DO 303 J2=1,8
      IF(N.NE.0)GO TO 305
      ABL(I)=AL(J1,J2)*F1(J1,J2)*AXX+ABL(I)
  305 A(I)=AL(J1,J2)*F1(J1,J2)+A(I)
  303 CONTINUE
   22 CONTINUE
      IF(N.EQ.0)GO TO 306
      RETURN
  306 CONTINUE
      IF(ABS(HACOS).NE.HASIN)GO TO 313
      DO 314 JKK=1,8
  314 ABL(JKK)=A(JKK)/2.
  313 CONTINUE
      DO 307 I=1,8
  307 A(I)=A(I)-ABL(I)
      RETURN
      END
C
C
C
      SUBROUTINE NZERO(KKK)
C
C
C
      REAL*8 H,I,J,K,L,M,N,P,Q,R,S,T,U,V,W,X
      REAL*8 XGAM1,XGAM2,XGAM3,XGAM4,XGAM5,XGAM6,A1,A2,A3,A4,A5,A6,A7,
     $A8,A9,A10,A11,A12,A13,A14,A24,A16,A17,A18,A19,A20,A21,A22,A23,A
      COMPLEX*16 Y,B,C,D,E,F,G,XX(8),TT,ZZ(8),C1,C2
      COMMON Y,B,C,D,E,F,G,H,I,J,K,L,M,N,P,Q,R,S,T,U,V,W,X
      COMMON ZZ
      COMMON XGAM1,XGAM2,XGAM3,XGAM4,XGAM5,XGAM6
      COMMON/AREA1/C1(10,8),C2(10,8),XX,TT
      A=Y
      XGAM5=N*R-P*Q
      XGAM6=N*T-P*S
      A1=H*U-K*A
```

```
362           A2=R*S-Q*T
363           A3=M*R-L*T
364           A5=L*S-M*Q
365           A6=N*M-K*S
366           A7=M*A-J*U
367           A8=P*M-K*T
368           A9=S*W-V*T
369           A10=-A2
370           A11=Q*W-V*R
371           A12=W*L-U*R
372           A13=W*M-T*U
373           A14=A9
374           A16=W*N-V*P
375           A17=L*P-K*R
376           A18=I*M-L*J
377           A19=I*U-L*A
378           A20=L*N-K*Q
379           A23=K*J-M*H
380           A24=I*K-L*H
381           TT=(0.,0.)
382           DO 58 II=1,8
383        58 XX(II)=(0.,0.)
384           DO 4 II=1,10
385           DO 4 JJ=1,8
386           C2(II,JJ)=(0.,0.)
387         4 C1(II,JJ)=(0.,0.)
388           C1(1,1)=F
389           C1(2,1)=D
390           C1(3,1)=E
391           C1(4,1)=C
392           C1(5,1)=G
393           C1(6,1)=B
394           DO 21 II=1,6
395        21 C1(II,2)=(1.,0.)
396           DO 9 II=1,8
397         9 XX(II)=(0.,0.)
398           CALL CALC(2,3,2,10)
399           DO 10 II=1,8
400        10 C1(10,II)=C2(10,II)*Y
401           DO 1 II=1,8
402         1 XX(II)=(0.,0.)
403           XGAM1=-K*A2-L*XGAM6+M*XGAM5
404           XGAM2=U*XGAM6+V*A8-W*A6
405           XGAM3=-U*A2+V*A3+W*A5
406           TT=A2*K*(A1*A2 +A*(P*A5+N*A3) +H*(M*A11-A9*L))+XGAM5*(M*A*(2.*L*
407          $ XGAM6-R*A6)+A3*(J*N*U+H*V*M)+J*S*U*A17+Q*A7*A8)+XGAM6*L*(A*(A17*S
408          $-T*A20)+I*U*XGAM6+I*(K*A14-M*A16))+A3*N*(Q*(    -A13*H)+A12*H*S)
409           TT=TT+XGAM1*(J*(K*A11-L*A16    )-XGAM2*I)-I*L*XGAM2*XGAM6+
410          $XGAM3*S*L*P*H+M*P*Q*H*(-W*A5+U*A2)
411           TT=TT+A3*(-H*L*N*V*T)
412           XX(1)=TT
413           TT=A6*(S*A1+N*A7+V*A23)
414           CALL CALC(1,2,2,1)
415           TT=A8*(T*A1+P*A7+W*A23)
416           CALL CALC(3,2,2,2)
417           TT=-A5*(S*A19+Q*A7-V*A18)
418           CALL CALC(1,4,2,3)
419           TT=A3*(T*A19+R*A7-W*A18)
420           CALL CALC(3,4,2,4)
421           TT=A20*(Q*A1-N*A19+V*A24)
```

```
      CALL CALC(1,5,2,5)
      TT=A2*(A*A2-I*A14+J*A11)
      CALL CALC(6,4,2,6)
      TT=A17*(R*A1+W*A24-P*A19)
      CALL CALC(3,5,2,7)
      TT=XGAM6*(A*XGAM6+H*A14-J*A16)
      CALL CALC(6,2,2,8)
      TT=XGAM5*(XGAM5*A+H*A11-I*A16)
      CALL CALC(5,6,2,9)
      DO 5 II=1,9
      DO 5 JJ=1,8
    5 C1(II,JJ)=C2(II,JJ)
      TT=A19*L
      CALL CALC(3,7,4,2)
      TT=A1*K
      CALL CALC(1,7,4,1)
      TT=(J*V-S*A)*S
      CALL CALC(1,6,4,3)
      TT=(J*W-T*A)*T
      CALL CALC(2,6,4,4)
      TT=(V*I-Q*A)*Q
      CALL CALC(5,6,4,5)
      TT=(I*W-R*A)*R
      CALL CALC(7,6,4,6)
      TT=(H*V-N*A)*N
      CALL CALC(5,8,4,7)
      TT=-A7*M
      CALL CALC(2,3,4,8)
      TT=(W*H-P*A)*P
      CALL CALC(9,2,4,9)
      DO 3 II=1,8
    3 C1(5,II)=C2(5,II)
      TT=(1.,0.)
      CALL CALC(5,10,6,1)
      DO 2 II=1,8
    2 ZZ(II)=XX(II)*(-1.,0.)
      RETURN
      END
C
C
C
      SUBROUTINE ZERO(JK)
C
C
C
      REAL*8 H,I,J,K,L,M,N,P,Q,R,S,T,U,V,W,X
      COMPLEX*16 C1,C2,X1,X2,X3,X4,X5,X6,XX(8),TT,ZZ(8),A,B,C,D,E,F,G
      REAL*8 XGAM1,XGAM2,XGAM3,XGAM4,XGAM5,XGAM6,A1,A2,A3,A4,A5,A6,A7,
     $A8,A9,A10,A11,A12,A13,A14,A15,A16,A17,A18,A19,A20,A21,A22,A23,A24
      REAL*8 A25,A26,A27,A28,A29,A30,A31,A32,XGAM7
      COMMON A,B,C,D,E,F,G,H,I,J,K,L,M,N,P,Q,R,S,T,U,V,W,X
      COMMON ZZ
      COMMON XGAM1,XGAM2,XGAM3,XGAM4,XGAM5,XGAM6
      COMMON/AREA1/C1(10,8),C2(10,8),XX,TT
      XGAM5=P*Q-N*R
      A1=T*N-P*S
      A5=Q*T-R*S
      A15=L*T-M*R
      A16=M*P-K*T
      A17=L*S-M*Q
```

```
482           A18=M*N-K*S
483           A22=H*S-J*N
484           A24=P*J-H*T
485           A26=I*T-R*J
486           A28=J*K-H*M
487           A30=I*M-J*L
488           A32=I*S-J*Q
489           IF(JK.EQ.0.)GO TO 1
490           U=J
491           V=M
492           W=S
493           X=T
494           A4=-A5
495           A6=-A15
496           A7=A17
497           A8=-A18
498           A9=A16
499           A10=A1
500           A11=-A26
501           A12=-A32
502           A13=A24
503           A14=-A22
504           A23=A13
505           A25=A26
506           A29=A28
507           A31=A30
508         1 CONTINUE
509           A2=L*P-K*R
510           A3=K*Q-N*L
511           A19=R*H-P*I
512           A21=Q*H-I*N
513           A27=H*L-I*K
514           IF(JK.EQ.1)GO TO 2
515           A4=R*W-Q*X
516           A6=V*R-L*X
517           A7=L*W-V*Q
518           A8=K*W-V*N
519           A9=V*P-K*X
520           A10=X*N-P*W
521           A11=R*U-I*X
522           A12=U*Q-I*W
523           A13=U*P-H*X
524           A14=U*N-H*W
525           A23=U*P-H*X
526           A25=I*X-U*R
527           A29=U*K-H*V
528           A31=I*V-U*L
529         2 CONTINUE
530           A20=-A10
531           XGAM1=-U*A2-H*A6+I*A9
532           XGAM2=H*A7-I*A8+U*A3
533           XGAM3=-Q*A13-I*A10+R*A14
534           XGAM6=-J*A2+H*A15+I*A16
535           XGAM7=H*A17+I*A18+J*A3
536           TT=(0.,0.)
537           DO 58 II=1,8
538        58 XX(II)=(0.,0.)
539           DO 20 II=1,10
540           DO 20 JJ=1,8
541           C1(II,JJ)=(0.,0.)
```

```
      20 C2(II,JJ)=(0.,0.)
         C1(1,1)=C
         C1(2,1)=D
         C1(3,1)=A
         C1(4,1)=B
         C1(5,1)=E
         C1(6,1)=F
         C1(7,1)=G
         DO 21 II=1,10
      21 C1(II,2)=(1.,0.)
         CALL CALC(3,4,2,1)
         CALL CALC(6,3,2,2)
         CALL CALC(3,5,2,3)
         CALL CALC(6,4,2,4)
         CALL CALC(5,4,2,5)
         CALL CALC(6,5,2,6)
         CALL CALC(3,2,2,9)
         CALL CALC(6,2,2,10)
         X1=L*A1*(W*A2+X*A3-V*XGAM5)+A5*K*(K*A4-N*A6-P*A7)+M*XGAM5*(-R*A8
        $-Q*A9-L*A10)
         X2=XGAM3*XGAM5*J+H*A5*(H*A4-N*A11+P*A12)+I*A1*(-I*A10-Q*A13+R*A14)
         X3=-XGAM1*XGAM6
         X4=-XGAM2*XGAM7
         DO 52 II=1,8
      52 XX(II)=(0.,0.)
         XX(1)=X1*A+X2*B+X3*E+X4*F
         XX(2)=X1+X2+X3+X4
         X1=-A20*A1
         X2=-A18*A8
         X3=A16*A9
         X4=-A22*A14
         X5=A23*A24
         X6=A28*A29
         DO 26 JJ=1,8
      26 C1(10,JJ)=X1*C2(1,JJ)+X2*C2(2,JJ)+X3*C2(3,JJ)+X4*C2(4,JJ)+X5*C2
        $ (5,JJ)+X6*C2(6,JJ)
         TT=(1.,0.)
         CALL CALC(2,10,3,7)
         X1=-A4*A5
         X2=A17*A7
         X3=-A6*A15
         DO 27 JJ=1,8
      27 C1(10,JJ)=X1*C2(1,JJ)+X2*C2(2,JJ)+X3*C2(3,JJ)
         TT=(1.,0.)
         CALL CALC(1,10,3,7)
         DO 7 II=9,10
         DO 7 JJ=1,8
       7 C1(II,JJ)=C2(II,JJ)
         DO 8 II=4,6
         DO 8 JJ=1,8
       8 C1(II,JJ)=C2(II,JJ)
         TT=-A32*A12
         CALL CALC(1,4,3,8)
         TT=A25*A26
         CALL CALC(1,5,3,9)
         TT=A30*A31
         CALL CALC(1,6,3,10)
         DO 9 II=1,8
       9 C1(3,II)=C2(9,II)
         X1=M*V
```

```
602            X2=S*W
603            X3=T*X
604            X4=U*J
605            DO 10 II=1,8
606           10 C1(4,II)=C2(10,II)*X1+C2(8,II)*X2
607            TT=(-1.,0.)
608            CALL CALC(4,9,5,7)
609            DO 11 II=1,8
610           11 C1(5,II)=C1(9,II)*X3+C1(10,II)*X4
611            TT=(-1.,0.)
612            CALL CALC(3,5,5,7)
613            IF(JK.EQ.0)GO TO 22
614            X1=A2*A2
615            X2=A19*A19
616            X3=A3*A3
617            X4=A21*A21
618            X5=XGAM5*XGAM5
619            X6=A27*A27
620            DO 12 II=1,8
621           12 C1(4,II)=X1*C2(3,II)+X2*C2(5,II)+X3*C2(2,II)+X4*C2(4,II)+X5*
622             $C2(1,II)+C2(6,II)*X6
623            TT=(1.,0.)
624            CALL CALC(4,7,3,7)
625            DO 13 II=1,8
626           13 ZZ(II)=XX(II)
627            X1=N*N
628            X2=P*P
629            X3=K*K
630            DO 14 II=1,8
631           14 C1(5,II)=X1*C2(4,II)+X2*C2(5,II)+X3*C2(6,II)
632            CALL CALC(5,9,4,7)
633            X1=R*R
634            X2=Q*Q
635            X3=L*L
636            DO 44 II=1,8
637           44 C1(3,II)=(0.,0.)
638            C1(3,1)=A
639            C1(3,2)=(1.,0.)
640            DO 15 II=1,8
641           15 C1(5,II)=C2(9,II)*X1+X2*C2(8,II)+C2(10,II)*X3
642            CALL CALC(5,3,4,6)
643            CALL CALC(9,1,3,4)
644            DO 38 II=1,8
645           38 C1(10,II)=C2(5,II)
646            C1(6,1)=F
647            C1(6,2)=(1.,0.)
648            C1(6,3)=(0.,0.)
649            CALL CALC(6,10,3,10)
650            DO 40 II=1,8
651           40 C1(10,II)=C2(10,II)
652            X1=H*H
653            X2=I*I
654            DO 16 II=1,8
655           16 C1(5,II)=(-1.,0.)*C2(4,II)+C1(2,II)*X1+C1(1,II)*X2
656            CALL CALC(5,10,6,5)
657            DO 17 II=1,8
658           17 C1(4,II)=C2(5,II)+C2(7,II)+C2(6,II)
659            DO 23 II=1,8
660           23 XX(II)=ZZ(II)
661            TT=(-1.,0.)
```

```
662           CALL CALC(4,7,7,4)
663        22 CONTINUE
664           DO 25 II=1,8
665        25 ZZ(II)=XX(II)*(-1.,0.)
666           RETURN
667           END
668     C
669     C
670     C
671           SUBROUTINE CALC(L,K,M,KK)
672     C
673     C
674     C
675           COMPLEX*16 C1,C2,XX,TT
676           COMMON/AREA1/C1(10,8),C2(10,8),XX(8),TT
677           DO 4 I=1,8
678         4 C2(KK,I)=(0.,0.)
679           KR=M+2
680           DO 2 N=2,KR
681           DO 1 I=1,8
682           DO 3 J=1,8
683           IF(I.GE.N) GO TO 2
684           IF(I+J.NE.N)GO TO 3
685           C2(KK,N-1)=C2(KK,N-1)+C1(L,J)*C1(K,I)
686           GO TO 1
687         3 CONTINUE
688         1 CONTINUE
689         2 XX(N-1)=C2(KK,N-1)*TT+XX(N-1)
690           RETURN
691           END
692     C
693     C
694     C
695           SUBROUTINE CHECK(I)
696     C
697     C
698     C
699           COMPLEX*16 DX
700           COMPLEX*8 DDX
701           REAL*8 STORE
702           COMPLEX*16 F1,XRET,F2(8,8)
703           COMMON/AREA2/F1(8,8),XRET(36,7),STORE(36,16)
704           IF(I.EQ.0) GO TO 6
705           DO 12 N1=1,8
706           DO 12 N2=1,8
707        12 F2(N1,N2)=(0.,0.)
708           F2(1,1)=XRET(8,2)
709           F2(1,2)=STORE(1,4)
710           F2(1,3)=STCRE(1,10)
711           F2(1,6)=STORE(1,8)
712           F2(1,7)=STCRE(1,3)
713           F2(2,4)=STORE(1,1)
714           F2(2,5)=STCRE(1,2)
715           F2(2,8)=F2(1,7)
716           F2(3,4)=F2(1,2)
717           F2(3,5)=STORE(1,5)
718           F2(3,8)=F2(2,5)
719           F2(4,6)=F2(3,5)
720           F2(4,7)=F2(1,6)
721           F2(5,6)=F2(1,2)
```

```
      F2(5,7)=F2(1,3)
      F2(6,8)=F2(2,4)
      F2(7,8)=F2(1,2)
      F2(8,8)=XRET(1,7)
      DO 16 N2=1,6
      N3=N2+1
   16 F2(N3,N3)=XRET(7,N2)
      DO 13 N2=1,8
      DO 13 N1=1,8
   13 F2(N1,N2)=F2(N2,N1)
      DO 14 N1=1,8
      DO 14 N2=1,8
      DX=(0.,0.)
      DO 15 N3=1,8
   15 DX=DX+F2(N1,N3)*F1(N3,N2)
      DDX=DX
      CX=AIMAG(DDX)
      EX=REAL(DDX)
   14 WRITE(6,2002)CX,EX
 2002 FORMAT(' ',E14.7,3X,E14.7)
    6 RETURN
      END
END OF FILE
```

Appendix IV The Effect of More Distant Nuclei in the Ruderman-Kittel Model

We use the approximate lineshape of an $\underline{X}A$ configuration for the determination of the effect of more distant nuclei. If $J_{AX} << W_X$, the $\underline{X}A$ spectrum is Lorentzian and is equal to (43) of section II except that $2W_X$ is replaced by

$$2W_X + 7(\pi J_{AX})^2/20W_X \tag{1}$$

(D.G. Hughes, private communication). To take into account the effect of the more distant nuclei we assume that the apparent increase in the relaxation rate of the observed nucleus due to each of the more distant unlike magnetic nuclei is equal to $7(J_{AX}\pi)^2/40W_X$ and that the increases add linearly. This is equivalent to assuming that the more distant nuclei are independent of each other. Then the apparent increase in the relaxation rate of a Sn^{117} nucleus is

$$\begin{aligned}&(7/40W_X)^2\Sigma_i(\pi J_{iX})^2 p_{un} \\ &= (7/40W_X)\pi^2 J_1^2 \Sigma_i F(k_f|R_{iX}|)^2 p_{un}/.7705\times10^{-6} = 3.3825 J_1^2 p_{un}/2\end{aligned} \tag{2}$$

Here the sum Σ_i is over all nuclear sites outside the 3 inner shells. Also J_1 is the magnitude of the Ruderman-Kittel interaction for nearest neighbours, $F(x)$ is given in equation (34) and p_{un} is the probability of a magnetic nucleus (other than a Sn^{117} nucleus) being found at a lattice site. The result is that the apparent increase in the relaxation rate is

$$0.3054 J_1^2/2W_X . \tag{3}$$

We have not taken into account the effect of like nuclei nor the mu-

tual interactions between the more distant nuclei in the calculations leading to (3). Because (3) is an approximate expression for the effect of more distant nuclei, we multiply this expression by ξ and obtain for the apparent increase in W_X

$$\xi\{.3054J_1^2/2W_X\} \tag{4}$$

Here ξ is a fitting parameter and its magnitude is found by minimizing (2) of section IV.